

# Immunohistochemical study supports the targeting of HSP27 alone, or HSP27 in combination with AKT, as therapeutic strategies to treat SPARC+/*PTEN*-wt or SPARC+/*PTEN*-null gliomas

Laila M. Poisson<sup>1</sup>, Sandra Cottingham<sup>2</sup>, Aditya Raghunathan<sup>3</sup>, Andrea Transou<sup>4</sup>, Enoch Carlton<sup>4</sup>, Stacey L. Thomas<sup>4,5</sup> and Sandra A. Rempel<sup>4,5,\*</sup>

<sup>1</sup>Departments of Neurosurgery and Public Health Sciences, Henry Ford Hospital, Detroit, MI;

<sup>2</sup>Departments of Pathology and Clinical Neurosciences, Spectrum Health System, Grand Rapids, MI;

<sup>3</sup>Department of Pathology, Henry Ford Hospital, Detroit, MI;

<sup>4</sup>Barbara Jane Levy Laboratory of Molecular Neuro-Oncology, Hermelin Brain Tumor Center, Henry Ford Hospital, Detroit, MI;

<sup>5</sup>Laboratory of Molecular Neuro-Oncology, Division of Neurosurgery, Department of Clinical Neurosciences, Spectrum Health System, Grand Rapids, MI, USA.

## ABSTRACT

Secreted Protein Acidic and Rich in Cysteine (SPARC) promotes glioma migration and invasion, and does so, in part, by activating p38 mitogen activated protein kinase (P38 MAPK)–mitogen-activated protein kinase-activated protein kinase 2 (MK2)–heat shock protein 27 (HSP27) signaling. Phosphatase and tensin homolog (PTEN) suppresses SPARC-induced invasion, and decreases pAKT, serine (S)15- and S78HSP27. Therefore, SPARC function is affected by PTEN. Consequently, we propose targeting HSP27 in *PTEN*-wild-type gliomas, and both HSP27 and AKT in *PTEN*-null gliomas. Our *in vitro* studies support this therapeutic strategy; however, we do not know whether these pathways are reflected in human tumors. In this immunohistochemistry study, we examined SPARC, HSP27, and AKT expression and phosphorylation relative to tumor grade, to *PTEN* genetic status, to

tumor invasion, and to patient survival. The results show that all glioma grades have elevated SPARC and S82HSP27. The expression of HSP27, S15HSP27, and S78HSP27, AKT and phospho (p)AKT increases with increasing grade. We found that the loss of *PTEN* correlates with increased HSP27, S15HSP27, S78HSP27 and pAKT. Finally, we observed that increasing levels of SPARC and pAKT correlate with shorter patient survival, as does any expression of S78HSP27. This study provides important rationale for targeting HSP27 alone, or HSP27 and AKT together, to treat glioma patients.

**KEYWORDS:** glioblastoma, astrocytoma, SPARC, HSP27, PTEN, signaling pathways, therapeutic targets

## INTRODUCTION

Diffuse astrocytomas represent approximately 80% of malignant brain tumors. Historically, adult infiltrating gliomas were histologically classified as diffuse astrocytoma and oligodendroglioma, and were designated grades II-IV by criteria established by the World Health Organization (WHO), with glioblastoma (GBM) corresponding to a grade IV infiltrating astrocytoma [1]. Recent advances made

\*Corresponding author

8723 Vergennes St. SE, Ada, MI 49301, USA.  
sandra.rempel@mich.com

AR is at the Department of Laboratory Medicine and Pathology, Mayo Clinic, Rochester, MN. SAR is retired.

possible by The Cancer Genome Atlas (TCGA) have made significant contributions to molecular characterization related to gene expression and genetic and DNA methylation signatures [2, 3, 4], providing a wealth of information to assist investigators in their particular fields of study. Importantly, these recent advances have resulted in the 2016 revision of the WHO classification of central nervous system tumors [5].

While it is anticipated that these recent advances will provide new treatment options, GBM patients presently have a poor prognosis, largely due to the highly infiltrative/invasive nature of these tumors and their poor response to current treatment modalities. The median survival of newly diagnosed GBM patients is only 14.6 months following the standard of care treatment, which is surgery followed by treatment with temozolomide (TMZ) plus radiotherapy (RT), followed by 6 months of adjuvant TMZ treatment [6], depending on the O<sup>6</sup>-alkylguanine DNA alkyltransferase (MGMT) methylation status of the patient's tumor [7]. However, there is cause for concern that radiation therapy may, in fact, enhance the invasive phenotype of these tumors [8]. In addition, a dramatic infiltrative pattern was commonly associated with the failure of ongoing bevacizumab therapy [9]. Clearly, novel therapies that restrict glioma infiltration are necessary. We have therefore looked for genes that are involved in regulating the infiltrative/invasive phenotype.

Using subtractive hybridization of astrocytoma and glioblastoma cDNA libraries, we found overexpression of SPARC [10], also known as osteonectin [11] and BM-40 [12], in all grades of primary human infiltrating astrocytomas [13]. Increased SPARC transcript (average 9.4-fold) was also observed by Parsons *et al.* [14]. The data therefore indicate that SPARC upregulation is one of the earliest changes in glioma progression, and its expression remains regionally elevated.

We and others have demonstrated that this upregulation of SPARC enhances the malignant phenotype. SPARC promotes migration and invasion *in vitro* [15] and invasion *in vivo* [16, 17], and conversely, its downregulation inhibits migration and invasion [18]. We have further demonstrated that SPARC upregulates the P38 MAPK-MAPKAPK2 (MK2)-HSP27 signaling axis (see Figure 1), and that inhibiting HSP27 expression through HSP27 siRNA treatment blocks SPARC-induced migration and invasion [19]. We found that SPARC increases

total HSP27 and its phosphorylation at all three serine (S15, S78, and S82) residues [20, 21], and increases the phosphorylation of S78HSP27 relative to total HSP27 [20].

Interestingly, cytoplasmic unphosphorylated HSP27 exists in complex with P38 MAPK, MK2, and AKT [21]. AKT is an important mediator of cell survival [22], which is, in turn, regulated by PTEN. *PTEN* is a major tumor suppressor gene lost and mutated in 27%-36% of primary GBMs and is methylated in up to 88% of secondary infiltrating astrocytomas [14, 23, 24]. *PTEN* negatively regulates AKT by dephosphorylating PIP3, and its loss therefore leads to increased pAKT.

We have demonstrated that *PTEN* reconstitution suppresses SPARC-induced migration and invasion *in vitro* and *in vivo*, and this is accomplished, in part, by suppressing the AKT signaling pathway [25] (see Figure 1). As the occurrence of *PTEN* loss/mutation/methylation is relatively high in malignant

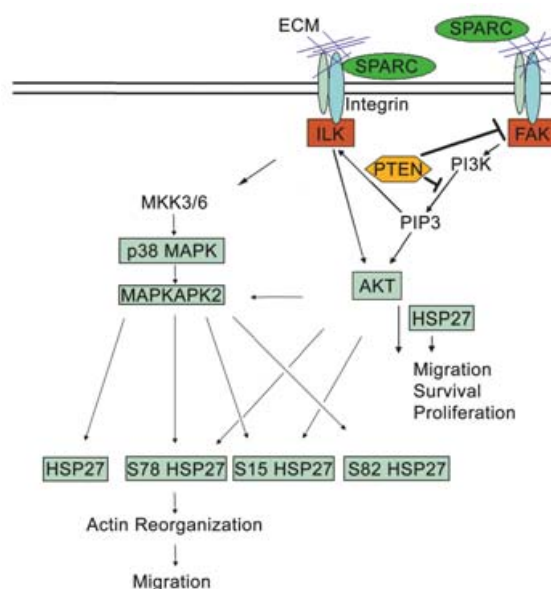


**Figure 1.** Proposed SPARC-mediated signaling pathways and regulation by PTEN. SPARC activates the p38 MAPK-MAPKAPK2 (MK2)-HSP27 signaling pathway to promote glioma tumor cell migration, possibly through integrin binding and ILK activation. AKT promotes phosphorylation of MK2 and HSP27 directly. PTEN suppresses glioma migration by dephosphorylation of PIP3, inhibiting AKT downstream signaling. (Adapted from Alam, R., Schultz, C. R., Golembieski, W. A., Poisson, L. M. and Rempel, S. A. 2013, *Neuro Oncol.*, 15(4), 451-461 with permission from Oxford University Press.)

glioma (27-36%), and at least 65% of tumors overexpress SPARC, there is a good chance that tumors express elevated levels of SPARC as well as mutant *PTEN*. The genetic background of infiltrating astrocytomas with respect to the expression of these two proteins may be important to consider as treatment strategies might differ depending on whether the tumors are SPARC+/*PTEN*-null versus SPARC+/*PTEN*-wild-type (wt). Therefore we examined the effects of pharmacologically suppressing HSP27 expression alone or in combination with AKT inhibition  $\pm$  temozolomide treatment. We reported that inhibiting HSP27 alone reduces tumor cell survival. When HSP27 inhibition was used in conjunction with pAKT inhibition in mutant *PTEN* tumor cells, survival was synergistically decreased, suggesting that *PTEN* status is important. Significantly, the combination treatment was more effective than temozolomide treatment alone [26], supporting the targeting of SPARC-induced signaling through HSP27 alone or with AKT inhibition (depending on *PTEN* status) as a therapeutic approach.

While we have significant *in vitro* and *in vivo* data supporting the use of this treatment strategy, we

do not know whether these pathways are reflected in human tumor specimens. In this study, we examined patients' samples to assess the relationship between SPARC, HSP27, and AKT protein expression, with respect to (a) glioma diagnosis and tumor grade, (b) *PTEN* status (wild-type or mutant/loss), (c) tumor invasiveness, and (d) patient survival. We thereby provide the necessary rationale to pursue these precision treatment strategies.

## MATERIALS AND METHODS

### Patients and tissue samples

Institutional Review Board (IRB)-approved informed consent was obtained from all patients to collect specimens used for this study, and IRB approval was obtained to perform this study. A total of 102 paraffin-embedded tumor tissue samples were used for immunohistochemistry analyses. A summary of clinical and molecular data is provided in table 1. Of the 102 tumors, 87 had frozen tissue samples that were submitted by Henry Ford Hospital to TCGA. Of these, 75 have known *PTEN* and *IDH* gene mutation status. These tumors were from

**Table 1.** Summary of clinical and molecular data.

Age at Diagnosis*	Median [min, max]	59 [23, 85]
Gender*	Male (%)	43/75 (57%)
	Female (%)	32/75 (43%)
Histology & Grade Diagnosis**	Astrocytoma, II (%)	6/102 (6%)
	Astrocytoma, III (%)	14/102 (14%)
	Glioblastoma, IV (%)	82/102 (82%)
MGMT Promoter** <sup>+</sup>	Methylated (%)	23/50 (31%)
	Unmethylated (%)	27/50 (36%)
IDH1/2*	Mutant (%)	9/75 (12%)
	Wild-type (%)	66/75 (88%)
Chromosomes 1p/19q*	Co-deleted (%)	0/75 (0%)
	Not Co-deleted (%)	75/75 (100%)
PTEN*	Mutant (%)	21/75 (28%)
	Homozygous deletion (%)	3/75 (4%)
	Wild-type (%)	51/75 (68%)

\*Molecular and clinical data taken from the pan-glioma TCGA paper (Ceccarelli *et al.*, Cell, 2016 [4]), of which 75 of our 102 cases are found.

\*\*An additional 27 Henry Ford Hospital cases were used for immunohistochemistry.

<sup>+</sup>25 of 75 GBM cases in this TCGA cohort did not have full assay of MGMT promoter methylation, so methylation status could not be determined.

32 female and 43 male patients, with an average age at diagnosis of 58.8 years. Thirty-five tumor specimens had tumor-adjacent brain tissue. Twenty-three independent brain specimens were obtained for use as normal controls. Upon histological review, two of these controls were excluded because major gliosis was observed. See supplementary databases S1 and S2 and supplementary table S1 for information on all patients and samples used for this study.

### Clinical data, tumor grading, and diagnosis

Complete clinical data, with available key molecular features, for the 87 tumors contained in TCGA were extracted from the supplemental files of the pan-glioma paper from TCGA [4] (see Supplementary database S2). This included histological diagnosis and grading as Grade II, Grade III or Grade IV infiltrating astrocytomas according to the WHO system [1]. For those 75 tumors with available somatic mutation and copy number variation data through TCGA, the new 2016 WHO classification of central nervous system tumors [5] was also applied. Histologic diagnosis and grade were taken from the clinical pathology report associated with the tissue for those cases not in TCGA.

### Molecular data

Putative copy number and mutation changes were downloaded from the cBioPortal through MSKCC ([www.cbioportal.org](http://www.cbioportal.org)) on February 11, 2016 and Oncoprint data on June 21, 2016. The pan-glioma data was also used (“merged Cohort of LGG and GBM; TCGA 2016”). An indicator of *PTEN* loss was constructed to represent either a somatic mutation in *PTEN* (any) or a substantial loss (a putative copy number call of -2); see supplementary database S2 and supplementary table S2.

### Immunohistochemistry

Paraffin-embedded tissue sections (5  $\mu$ m) were stained with hematoxylin and eosin (H&E) for histopathological evaluation. Immunohistochemical analysis was essentially performed as previously reported [13] after working out conditions and ensuring negative and positive control reproducibility in multiple runs (Supplementary figures S1 and S2). Briefly, formalin-fixed, paraffin-embedded 5  $\mu$ m tissue sections were subjected to routine deparaffinization and rehydration. Serial sections were subjected to

immunohistochemical detection for SPARC, HSP27, S15HSP27, S78HSP27, S82HSP27, PTEN, AKT and S473AKT using primary antibodies and methods described in supplementary table S3. Sections were blindly reviewed and scored by two neuropathologists. Each case was reviewed by one neuropathologist, with a subset reviewed by both to establish threshold. Staining intensity was graded as negative (0), weak (1), moderate (2), or strong (3). Percentage of tumor staining for a given antibody was scored as negative (0), less than 5% (1), 6-25% (2), 26-50% (3), 51-75% (4), and 76-100% (5).

### Statistical analyses

Heatmaps were used to simultaneously visualize protein intensity and percentage of tumor staining across multiple samples and proteins. In these grid diagrams, each row represents one measure (e.g., intensity in normal cells, intensity in tumor cells, or percentage of tumor cells staining) for one immunohistochemistry stain, and each column represents one case. Cases were ordered by clinical feature and then by intensity of total HSP27 within the tumor cell. Colors of increasing “heat” from green (low/“cold”) to red (high/“hot”) were used to symbolize increasing intensity or percentage. Exact tests, such as Fisher’s exact test, were used to compare counts of samples at each staining intensity between categories (e.g., grade). Bar charts were used to depict counts per intensity level, by category. As staining intensity is an ordinal measure, trend tests for change in proportions were also run to assess linear trends in the proportion of samples having a particular feature at each increasing intensity level. Overall survival is defined as the time from diagnosis to death (all cause), with patients who are still alive censored at the time of last contact. Progression free survival is defined as the time from diagnosis until the first evidence of tumor progression. Death is considered a progressive event if no other evidence is documented prior to death. Patients who are still alive without progression are censored at the time of last contact. Kaplan-Meier estimates were used in plots of survival curves between single predictors. Log-rank tests were used to compare these survival curves. Cox-regression models, assuming proportional hazards, were used to assess relationships between multiple predictors. All analyses were conducted in R, v3.2 (<http://www.cran.r-project.org/>).

## RESULTS

### Protein expression in independent normal and tumor-adjacent normal tissue

The intensity of staining of the independent normal and tumor-adjacent normal tissues, relative to that observed in the tumors, is shown as a heatmap in figure 2. Except for SPARC, the independent normal brain samples do not express (0), or have very little expression (1), of the proteins under consideration. In contrast, the tumor-adjacent normal samples tend to have higher levels of expression (3, 4); see also supplementary figure S3. The observation that tumor-adjacent normal brain is positive for SPARC is not surprising, as we have demonstrated that reactive astrocytes in normal brain adjacent to tumor express high levels of SPARC, as do the invading tumor cells [13]. As we show next, there is a close association between SPARC and HSP27 in all grades of infiltrating astrocytomas, and hence it is not surprising to see elevated (p)HSP27 in these tumor-adjacent normal tissues as well. In adult brain there are small populations of cells that normally express SPARC. These include the Bergmann glia in the cerebellum and marginal glia in the outer cortex [27]. We examined our independent normal specimens and found that the SPARC expression was detected in the Bergmann glia and/or reactive astrocytes in 19 of the 21 normal specimens (Supplementary database S1).

### Protein expression in tumors relative to tumor grade

Histologically, all 102 tumor specimens were identified to have astrocytic origin, though one tumor was classified as an oligoastrocytoma upon review by TCGA. There are 82 Grade IV tumors (GBM, 80.4%), 14 Grade III tumors (13.7%), and 6 Grade II tumors (5.9%). As expected from our previous study [13], SPARC is highly expressed in all grades of glioma, as is S82HSP27 (Figure 3). Expression levels of HSP27, S15HSP27, S78HSP27, AKT, and pAKT all significantly increase with increasing grade (Figure 3). The heatmap (Figure 2) also illustrates that as the staining intensity increases the percentage of tumor staining also increases. These results support our *in vitro* and *in vivo* studies that SPARC increases HSP27 expression and phosphorylation. However, when comparing the intensity of these proteins within each grade, there

are SPARC-expressing tumors that do not correlate with enhanced or phosphorylated HSP27 signaling (Figure 2). In accordance with our signaling model, this would be expected if these tumors were *PTEN*-wild-type, with consequent suppression of pAKT and downstream suppression of pHSP27. Therefore, we next examined the *PTEN* status of the specimens.

### Protein expression relative to *PTEN* status

With respect to *PTEN* genomic loss, only 8 (11%) of the 75 tumors were assumed to be diploid. Most had some loss (85% have putative call of -1) and three (4%) had substantial loss (putative call of -2). *PTEN* deactivation arises through either a substantial loss or mutation, but rarely both; see supplementary figure S4A. We therefore combined mutation (any) and loss (-2) to form a *PTEN* loss indicator. Of the 24 cases with *PTEN* loss, 3 are due to copy number loss and 21 are due to mutation; see supplementary table S2. To determine whether *PTEN* expression might correlate with inhibition of the SPARC-signaling pathway, the expression of each protein was compared between *PTEN*-wild-type and *PTEN*-null groups (Figure 4 and Supplementary figure S5). Genetic data was used because the *PTEN* antibody was detecting mutant *PTEN* protein as well as the wild-type protein, and consequently, the immunohistochemical signal intensity was not a reliable marker for *PTEN* functional status. This can be seen in figure 4 where there is no evidence of a difference in proteins between *PTEN*-loss and *PTEN*-wt tumors,  $p = 0.2374$ ; see also supplementary table S4.

The bar graphs (Figure 4) show that genomic loss of *PTEN* did not correlate with SPARC or S82HSP27 expression levels; however, it does correlate with significant increases in HSP27, S15HSP27, S78HSP27, and S473AKT. This suggests that *PTEN*, if present, could influence SPARC-induced upregulation of HSP27 by suppression of pAKT (Figure 1). Examining the associations between pAKT and the phosphorylations of HSP27 in *PTEN*-wild-type versus *PTEN*-null tumors (Table 2), we find that in *PTEN*-null tumors, pAKT correlates with S15HSP27; whereas this association is lost in *PTEN*-wild-type tumors. For the phosphorylated forms of HSP27, the strongest association is between S15- and S78HSP27. These data would support our

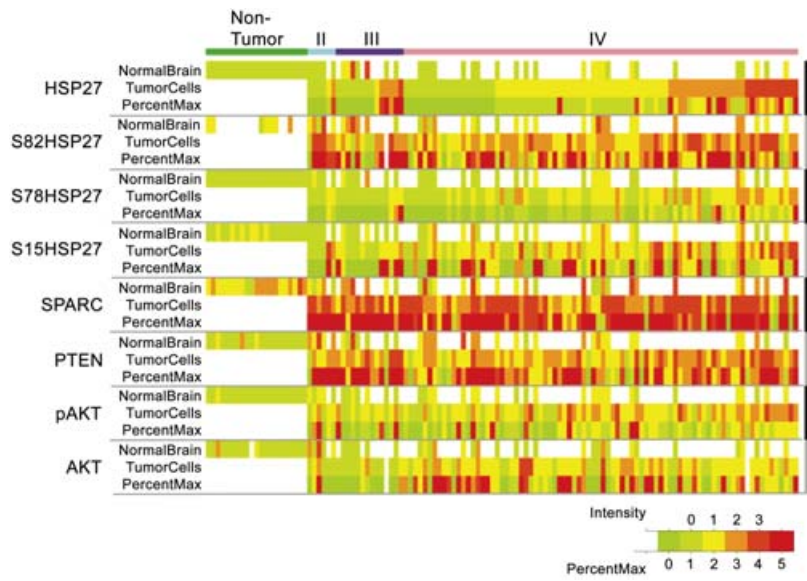


Figure 2

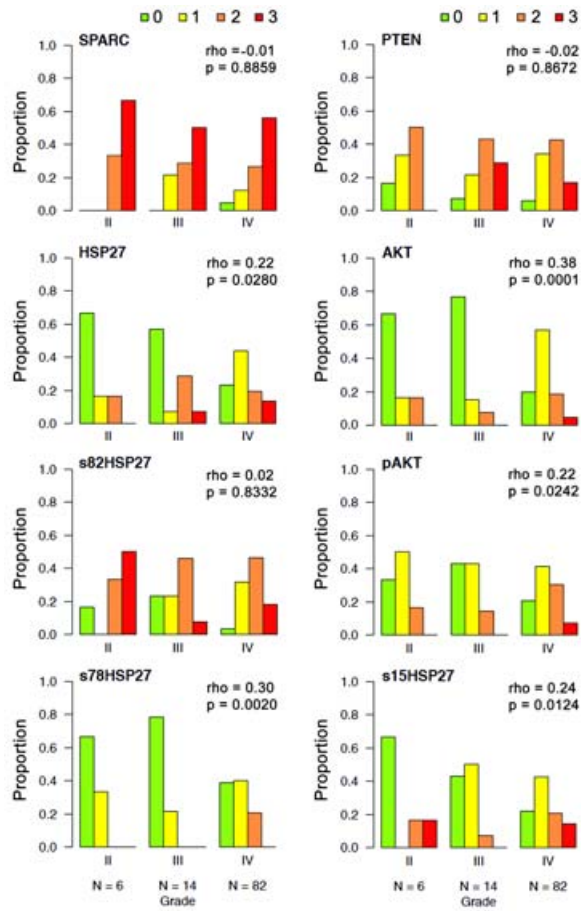


Figure 3

model to suggest that, in the absence of *PTEN*, increased pAKT phosphorylates serine 15 on HSP27 and this enhances phosphorylation on serine 78. When *PTEN* is present, pAKT is decreased. As a result, S15HSP27 is decreased, which would negatively impact the phosphorylation on serine 78. These data are in agreement with our published *in vitro* data that shows that *PTEN* reconstitution suppresses S15HSP27 and S78HSP27 in SPARC-expressing cells [20], and our *in vivo* data showing that *PTEN* suppresses growth and invasion of SPARC-expressing tumors [25].

To further assess the relevance of *PTEN* status, we considered whether our subset of tumors within the TCGA was representative of the tumors comprising the entire TCGA database, with a focus on *SPARC*, HSP27 (gene symbol:*HSPB1*), *PTEN* and *IDH*, the last two having been found to be virtually mutually exclusive genetic mutations, important in defining glioma subsets [4, 5].

#### ***PTEN* and *IDH* genetic status**

Within the 1084 TCGA glioma cases with whole genome sequencing, *IDH1* was the most commonly altered gene and *PTEN* was the fourth most commonly altered gene, (Supplementary figure S4A). Identified mutations for *PTEN* spanned the entire gene region (Supplementary figure S4B). Overall, *PTEN* was lost in 15% of the cases either through deep deletion or mutation. Loss of *PTEN* is nearly perfectly mutually exclusive of having an *IDH1/IDH2* mutation ( $p < 0.0001$ ).

Within the 75 Henry Ford Hospital (HFH) TCGA cases (63 GBM, 10 AA, 2 LGA), mutations in *PTEN* are primarily truncating or missense, with only three points being mutated in more than one sample

(Supplementary figure S4A, B). Mutations are primarily in the two functional domains (dual specificity phosphatase, catalytic domain or C2 domain). The mutation or wild-type status for *PTEN* and *IDH* for each tumor is indicated in supplementary database S2.

There is no evidence that *PTEN* mutation rate differs by grade ( $p = 0.6056$ ; Supplementary table S5); whereas, as expected from the global data in cBioPortal, the *PTEN* mutation is exclusive of an *IDH* mutation (FET  $p = 0.0545$ ; Supplementary table S6) in our tumor subset. There is a suggestion that *IDH* mutation is less likely with increasing grade (FET  $p = 0.0903$ ; Supplementary table S7). If the order of grade is accounted for in a trend test, the change in proportions is still not quite statistically significant (trend-test  $p = 0.0688$ ; Supplementary table S7). There was no correlation between elevated SPARC expression and *IDH* mutation ( $p = 0.2227$ ; Supplementary table S8). These combined data indicate that the subset of HFH tumors used for these analyses are representative of the larger set of glioma tumors in the TCGA database with respect to *PTEN* and *IDH* mutation rates.

As *IDH1* has become the primary diagnostic discriminator for diffuse infiltrating astrocytomas, we evaluated our staining results in the context of the new WHO classification system [5]. Of the 75 tumors under study that are profiled by TCGA, nine harbor an *IDH* mutation (9 *IDH1*, 0 *IDH2*) and none harbor a co-deletion of chromosomal arms 1p and 19q. By 2016 diagnostics, we have three “Diffuse Astrocytoma, *IDH*-mutant”, nine “Astrocytoma, *IDH*-wt, Diffuse Astrocytoma-NOS,” six “Glioblastoma, *IDH*-mutant,” and 57 “Glioblastoma, *IDH*-wt” tumors. As can be seen in figure 5, for GBMs, the increased

---

**Legend to Figure 2.** Heatmaps for HSP27, S82HSP27, S78HSP27, S15HSP27, SPARC, *PTEN*, S473AKT, and AKT. For each protein, the top heatmap is the maximum staining intensity in independent normal brain samples (NB; green) and tumor-adjacent normal brain (when present); the middle heatmap is the maximum staining intensity in the tumor cells; and the bottom heatmap is the percentage of tumor staining. Tissues are ordered first by grade (Non-Tumor, II, III, and IV) and then by HSP27. Intensity of staining is measured as 0 (none), 1, 2, or 3 (highest), and the percentage of tumor staining (PercentMax) is measured as 0 (none), 1, 2, 3, 4, or 5 (highest).

**Legend to Figure 3.** Barplots for SPARC, *PTEN*, HSP27, S82HSP27, S78HSP27, S15HSP27, S473AKT, and AKT. For each antibody, the barplots illustrate the proportion of samples at each staining intensity in the different grades of glioma samples. Levels of expression of HSP27, S78HSP27, S15HSP27, *PTEN*, AKT, and pAKT increase with increasing grade. SPARC, S82HSP27, and *PTEN* are high in all grades. Intensity of staining is measured as 0 (none), 1, 2, or 3 (highest). Significance is set at  $p \leq 0.05$ .

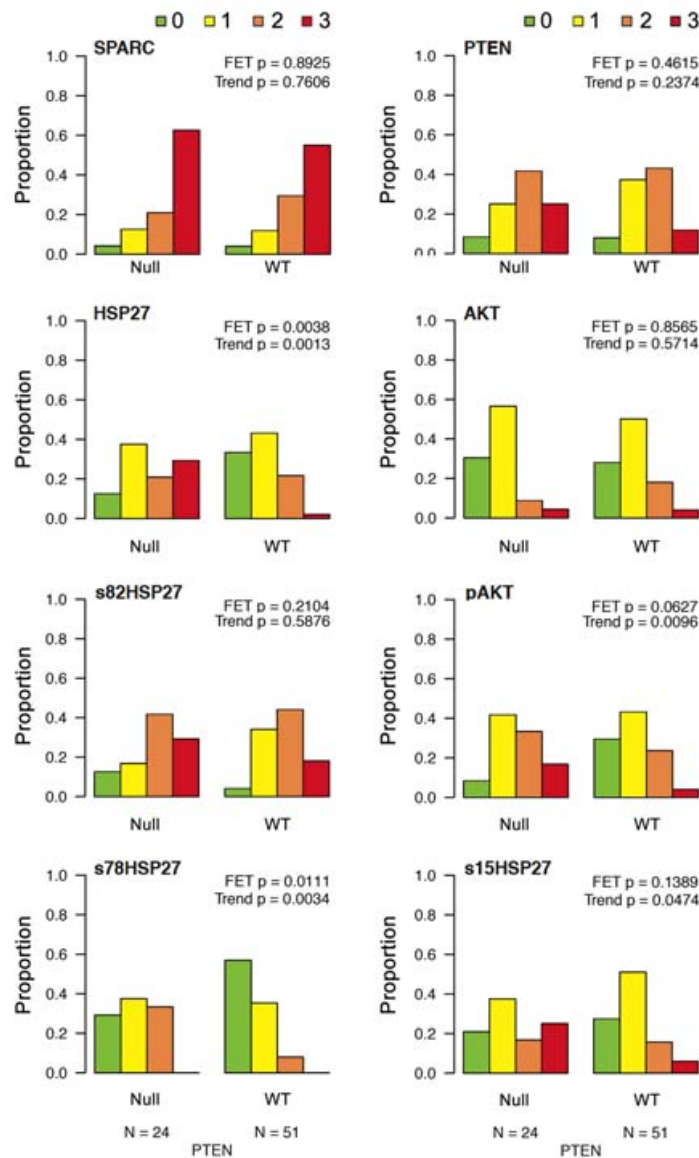


**Figure 4.** Barplots for SPARC, PTEN, HSP27, S82HSP27, S78HSP27, S15HSP27, S473AKT, and AKT. For each antibody, the barplots illustrate the proportion of samples at each staining intensity between those cases with *PTEN* (WT) and without (Null) *PTEN*. HSP27, S78HSP27, S15HSP27, and pAKT increase with the loss of *PTEN*. SPARC, S82HSP27, and AKT expression levels were not impacted by *PTEN* loss. *PTEN* staining did not correlate with *PTEN* genetic status indicating that the antibody detects mutant protein. Intensity of staining is measured as 0 (none), 1, 2, or 3 (highest). Significance is set at  $p \leq 0.05$ .

staining intensity of HSP27, S82HSP27, S78HSP27, S15HSP27, AKT, and pAKT increases with *IDH*-wt status in both the astrocytoma and GBM tumors. As our GBM *PTEN*-null tumors are *IDH*-wt, and those GBMs that are *IDH* mutant are *PTEN*-wild-type, the data are consistent between the 2007 and 2016 WHO classifications.

### Invasion

Our work has focused on the role of SPARC in promoting glioma migration and invasion. While immunohistochemistry of human specimens is vital to validate *in vitro* observations and results obtained through animal models, there is a significant shortfall with respect to the study of

**Table 2.** Correlation of protein expression.

PTEN-WT				
	S15	S78	S82	pAKT
S15	1.00	0.52	0.14	-0.02
S78		1.00	0.32	0.33
S82			1.00	0.33
pAKT				1.00
PTEN-Null				
	S15	S78	S82	pAKT
S15	1.00	0.66	0.47	0.39
S78		1.00	0.43	0.13
S82			1.00	0.17
pAKT				1.00

Spearman's correlation coefficients as a measure of the association between phosphorylation of HSP27 on serines 15, 78 or 82 and pAKT within PTEN-wild-type (WT) or PTEN-null tumors. A meaningful correlation is considered to occur at  $\geq 0.30$ .

glioma invasion. Most specimens do not have adjacent normal brain tissue, and when it is present, it is often not of sufficient size or volume to assess the role of a protein in invasion, let alone to perform serial sections examining a number of proteins. We were fortunate to have a single sample with sufficient adjacent normal tissue having invading tumor cells (Figure 6). We do not know the *PTEN* genetic status of this tumor to be able to comment on the pAKT staining. Nonetheless, we can see that SPARC expression correlates with increases in HSP27 and its phosphorylated forms, consistent with our *in vitro* studies.

### Survival

The overall survival (OS) curve for all patients in TCGA is illustrated in supplementary figure S4C. Also shown is the OS curve for the subset of patients used in this study. The OS curve is worse because the majority of patients in the HFH subset were patients with high-grade tumors.

For the HFH subset, we examined whether patient OS or progression-free survival (PFS) was influenced by SPARC, HSP27 and its phosphorylated forms, and total and pAKT, as measured by signal intensity. There was no significant difference in OS or PFS based on increasing level of intensity of HSP27, S82HSP27, S15HSP27, or AKT (see Supplementary figures S6-S12). However, we did see that

increasing intensity of SPARC was associated with worse OS and PFS (Figure 7). In addition, we found that OS and PFS were worse for patients with tumors expressing any S78HSP27, and that OS and PFS were worse with increasing pAKT.

We next examined whether *PTEN* presence or absence correlated with survival. We found no difference in survival between patients having tumors wild type for *PTEN* versus those having tumors mutant for *PTEN* (Supplementary figure S13). We found that PFS increased with increasing S78HSP27 in a *PTEN*-null background, whereas PFS increased with decreasing S78HSP27 in a *PTEN*-wild-type background (Figure 8). We found that OS and PFS decreased with increasing pAKT in both *PTEN*-null and *PTEN*-wild-type backgrounds. However, those tumors having no expression of pAKT had the worst survival (Figure 8). Looking at *PTEN* status and whether there was any correlation between any staining versus no staining, we see that the *PTEN* status discriminated between tumors having no expression versus any expression for both S78HSP27 and pAKT (Figure 8). The significance of this latter observation is not clear as the number of samples in the no staining/*PTEN*-null group is very small for both S78HSP28 ( $n = 6$ ) and for pAKT ( $n = 2$ ). A larger study specifically examining tumors with these genotypes is necessary. We found no association between *PTEN* status and OS and PFS survival relative to HSP27, S82HSP27, S15HSP27, and AKT expression (Supplementary figures S14-S19).

### DISCUSSION

In this study, we show that a large percentage of human glioma specimens express high levels of SPARC, HSP27 and its phosphorylated forms, and elevated AKT and pAKT. We also show a large percentage of tumors that, despite having high SPARC expression, do not have elevated levels of HSP27, S78HSP27, S15HSP27, AKT or pAKT. Importantly, we find a correlation between the loss of *PTEN* and enhanced HSP27, S15HSP27, S78HSP27, and pAKT. These results are critical because they substantiate our previous *in vitro* and *in vivo* studies indicating that *PTEN* can inhibit SPARC-induced upregulation of pAKT and the P38 MAPK-MK2-HSP27 signaling pathways. This provides further rationale to consider targeting HSP27  $\pm$  AKT (depending on *PTEN* status) as a therapeutic approach to treat glioma patients.

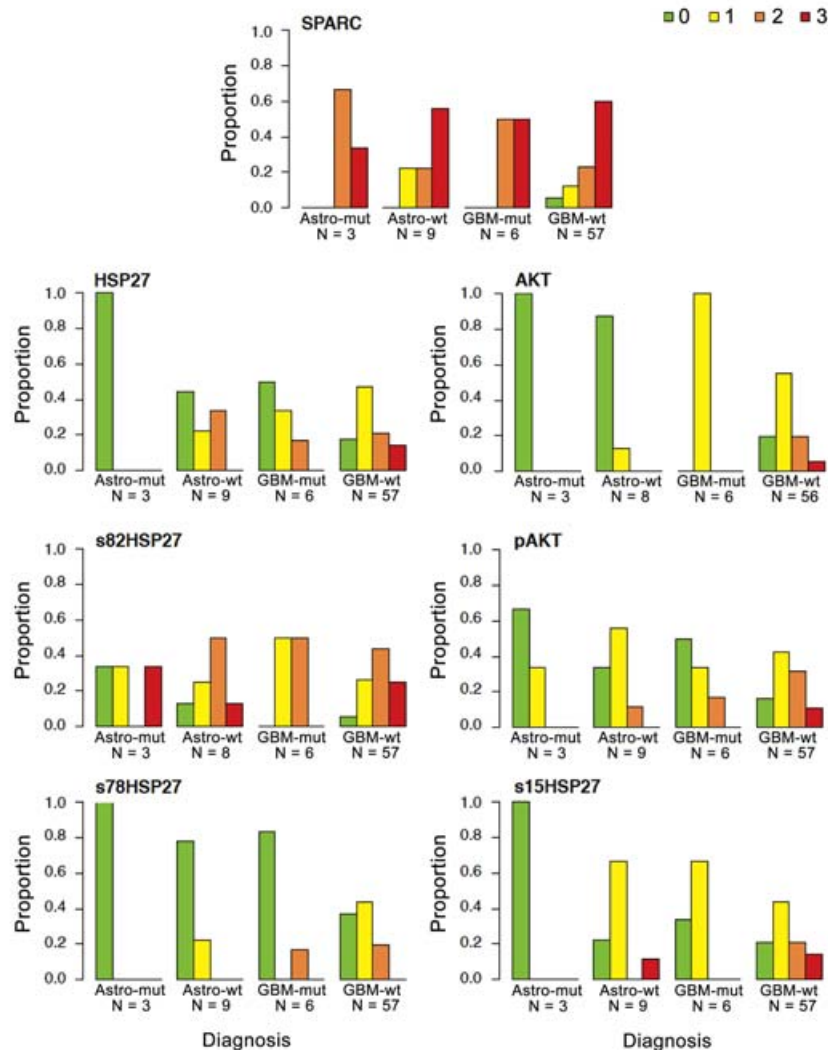


**Figure 5.** Barplots for SPARC, HSP27, S82HSP27, S78HSP27, S15HSP27, S473AKT, and AKT. For each antibody, the barplots illustrate the proportion of samples at each staining intensity between those cases diagnosed as diffuse astrocytoma, *IHD*-mutant (*Astro-mut*); diffuse astrocytoma, *IHD*-wild-type (*Astro-wt*); GBM, *IHD*-mutant (*GBM-mut*); and GBM, *IHD*-wild-type (*GBM-wt*). Intensity of staining is measured as 0 (none), 1, 2, or 3 (highest).

This study highlights the difficulties associated with not having truly normal brain tissues as controls for molecular studies, and reinforces the need to examine the expression of proteins directly in human brain tissue and tumor samples, where expression can be interpreted in the context of specific cells and associated pathologies. As a result, our studies show that SPARC is increased in the vast majority of tumors (96%), and its expression correlates with elevated pAKT and HSP27 and its phosphorylated forms in a large percentage of glioma specimens. It is important to point out that

specimens used as designated normal controls for brain tumor studies are rarely samples of truly normal brain. They are often brain tissue samples that are separately removed to gain access to tumor during surgery, and are designated as “normal brain”, but may indeed be compromised. Other normal brain specimens are brain tissue specimens removed in the treatment of other pathologies, such as epilepsy and brain metastases. Again, the normal brain may be compromised. The rationale for the use of these tissues as normal brain samples is two-fold. First, access to normal

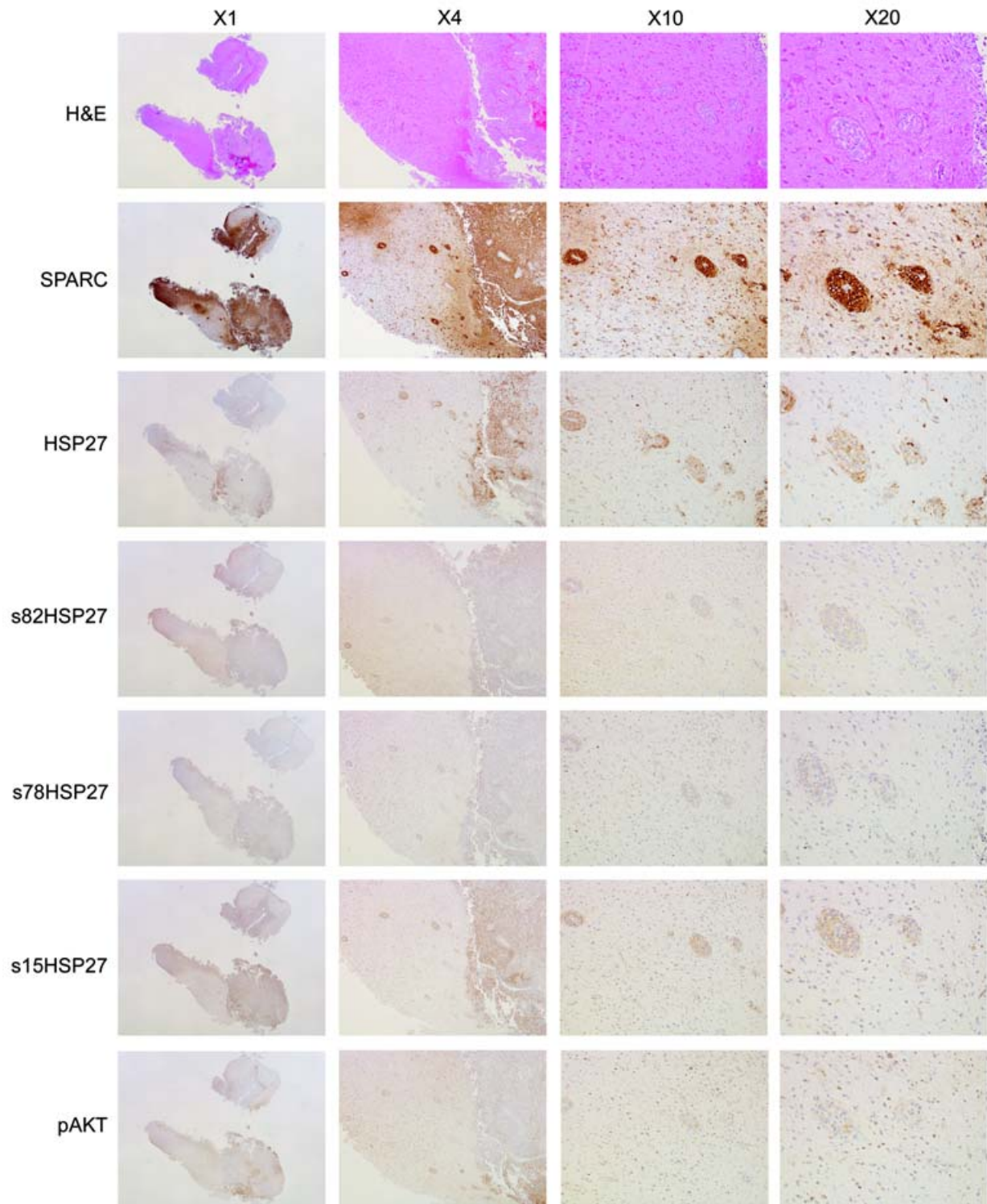


**Figure 6.** Serial sections of H&E and immunohistochemistry for the specimen HF2701. Staining is illustrated for HSP27, S82HSP27, S78HSP27, S15HSP27, SPARC and pAKT in the tumor cells at the invasive edge. High SPARC expression in the invading tumor cells was accompanied by increased HSP27, S82HSP27, S78HSP27, S15HSP27, and S473AKT. Magnifications are as indicated.

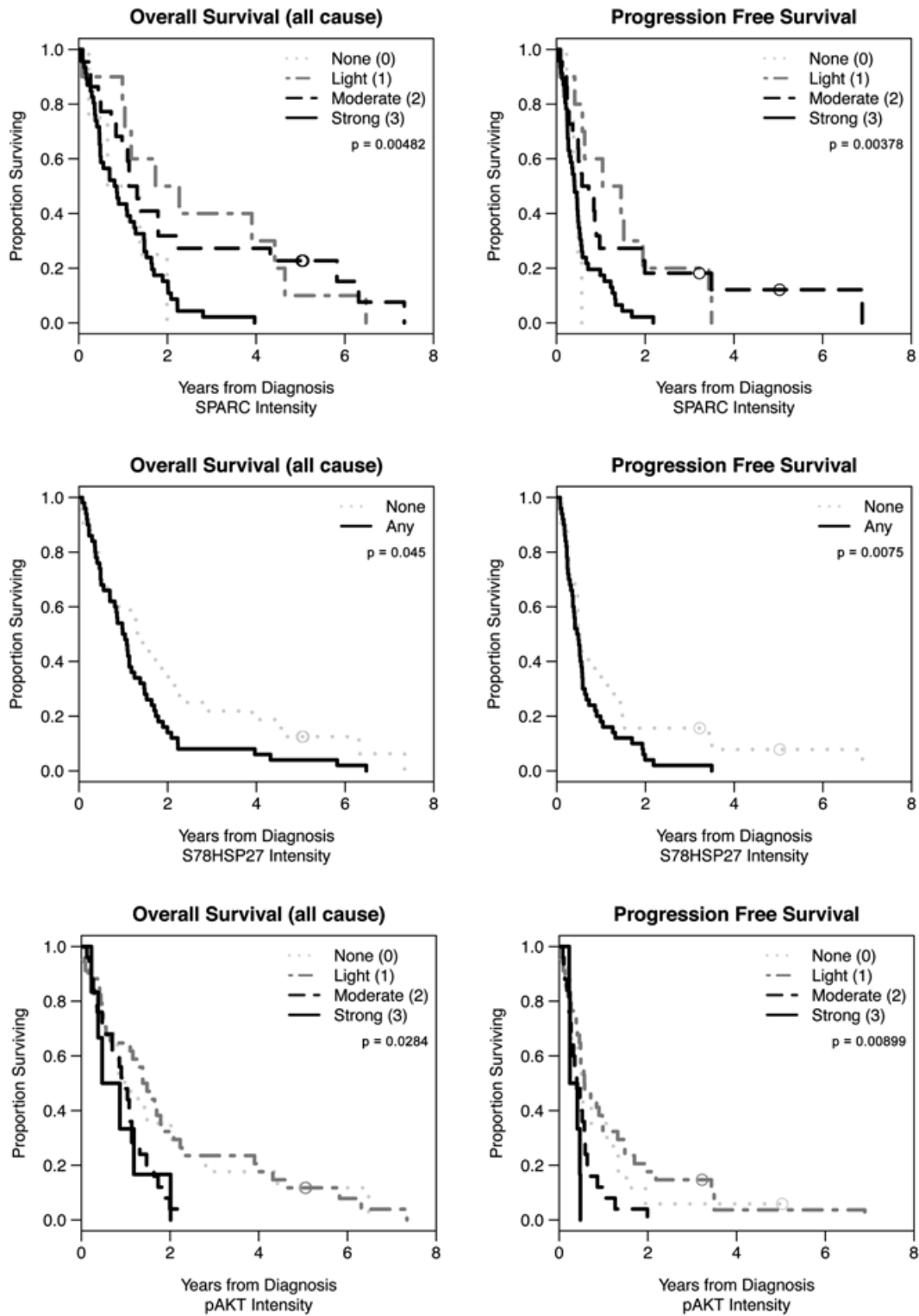


**Figure 7.** Patient survival relative to SPARC, S78HSP27 and pAKT staining. Kaplan-Meier plots showing overall survival and progression-free survival according to the intensity of SPARC staining (top panels), according to the presence or absence of S78HSP27 staining (middle panels), and according to the intensity of pAKT staining (bottom panels). Significance is set at  $p \leq 0.05$ .

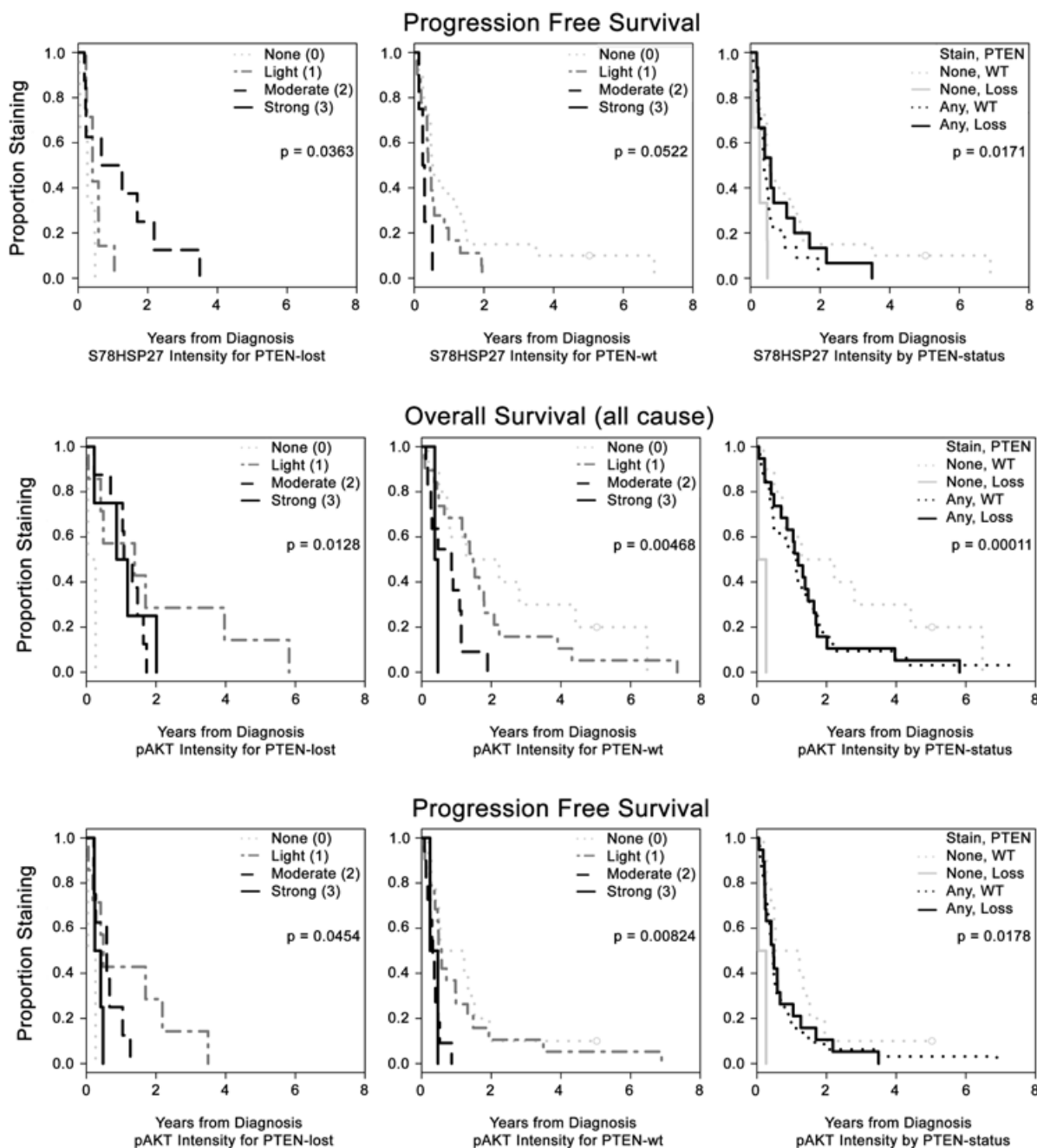


**Figure 8.** Patient survival relative to S78HSP27 and pAKT in the presence (*PTEN*-wt) or absence (*PTEN*-lost) of *PTEN*. Kaplan-Meier plots showing progression-free survival according to the intensity of S78HSP27 staining (top panels), overall survival according to the intensity pAKT staining (middle panels), and progression-free survival according to the intensity of pAKT staining (bottom panels). Significance is set at  $p \leq 0.05$ .

brain specimens is rare. Second, it is assumed that the genetic changes that result in cancer will be different from those involved in other pathologies. While this is a safe assumption for some genes, it may not be founded for others, such as SPARC

and other proteins, such as HSP27, that are more globally expressed in response to stress associated with many pathologies. As a result, the true increase in SPARC in glioma cells relative to normal brain is underrepresented in large databases such as

TCGA. By examining the cells expressing SPARC in the designated normal specimens, and eliminating the staining associated with normal SPARC expression in Bergmann glia cells and upregulated staining in reactive astrocytes that are associated with the underlying pathologies for those samples, our results show that SPARC is increased in tumors compared to normal cerebral cortex. As we have shown a close association between SPARC and HSP27, it is also not surprising to see elevated S82HSP27 in these designated normal tissues.

We next determined whether increased SPARC expression in the human tumors was associated with increased HSP27 and AKT expression and/or phosphorylation, and if so, whether this correlated with *PTEN* genetic status. We found that SPARC and S82HSP27 were elevated, and this was independent of *PTEN* status. Phosphorylation of HSP27 and AKT increased with increasing grade. Independent of grade, loss of *PTEN* correlated with increases in pAKT, S15HSP27, and S78HSP27. These *in vivo* correlations support our *in vitro* and *in vivo* observations.

To our knowledge, our study is the first comprehensive immunohistochemistry study of HSP27 and all three phosphorylated serine residues in infiltrating astrocytoma grades II-IV. Our results with HSP27 are in agreement with or are supported by other studies examining the expression of this protein and its phosphorylated forms in different glioma grades. In earlier studies, Klalid *et al.* [28] immunohistochemically examined 66 tumors (grades II-IV), and Hitotumatsu *et al.* [29] studied 48 tumors (grades II-IV). Both groups found increasing HSP27 expression with increasing grade. In another study, Strik *et al.* [30] found HSP27 expression in the majority of 44 infiltrating astrocytomas of different grade and histology; and an examination of 24 paired primary and recurrent GBMs by the same group showed HSP27 expression in the paired tumors [31]. More recently, Mälelä *et al.* [32] used tissue microarrays of 295 grade II-IV infiltrating astrocytomas to assess total HSP27, and found HSP27 expression associated with increasing grade. They did not look at phosphorylated HSP27. Alexiou *et al.* [33] examined 9 GBMs, and they found a significant positive correlation between S82HSP27 and S15HSP27 with increased total AKT. They did not examine S78HSP27. In agreement, we also found

that increasing HSP27 and its phosphorylation correlated with increased AKT and S473AKT.

We are particularly interested in examining the expression of the phosphorylated HSP27s, as HSP27 function changes depending on its phosphorylation status [34]. Using *PTEN* reconstitution to query SPARC-induced signaling through HSP27 upregulation and phosphorylation, we found that *PTEN* could inhibit SPARC-induced upregulation of pMK2 and S78HSP27 [20]. As our *in vivo* studies show, *PTEN* is capable of suppressing SPARC-induced tumor invasion [25]. These combined studies implicate SPARC-induced HSP27 phosphorylation on S78 with the invasive phenotype. The present study demonstrates a strong association of S78 with S15 and S82, suggesting phosphorylation at these sites may also contribute to the function of HSP27 in invasion.

One drawback to immunohistochemical studies is that it is difficult to relate intensity of expression of one protein relative to another because of inherent sensitivities of antibodies and variations in conditions used to gain access to epitopes that may render one phosphorylation site more accessible than others. It is also possible that phosphorylation at one or multiple sites may inhibit the binding of an antibody that detects unphosphorylated HSP27, which could lead to the false conclusion that no HSP27 is present. Therefore, it is interesting to note that for some tumors where total HSP27 is negative, there is still a signal for a phosphorylated form of HSP27. These results reinforce the need to look at total and phosphorylated HSP27.

Our research supports the contention that increased SPARC induces signaling through the upregulation of the P38 MAPK-MK2-HSP27 signaling axis, and this is augmented by the loss of *PTEN*. As we have evaluated SPARC signaling relative to tumor grade and specifically to *PTEN* signaling, we wondered if our data and interpretation of results would be impacted by the change in the WHO classification system. Interestingly, the major restructuring is based on *IDH* genetic status [5]. As it turns out, *PTEN* mutations rarely occur concurrently with *IDH* mutation in the same tumor. Indeed, in our tumor subset, they were mutually exclusive. Reclassifying our tumors according to the new WHO system, we found that the mutation of *IDH1* (*PTEN*-wild-type) correlated with lower expression of total and phosphorylated HSP27 and total and

pAKT. Interestingly, Mälelä *et al.* [32] also found that increasing HSP27 expression with increasing tumor grade correlated significantly with decreased percentage of tumors having *IDH1* mutation. Like *PTEN*, *IDH1* status had no correlation with SPARC expression. We could therefore include *IDH* status in our proposal to say that SPARC+/*PTEN*+/*IDH*-tumors should be therapeutically treated by targeting HSP27, whereas SPARC+/*PTEN*-/*IDH*+ tumors should be targeted for both pHSP27 and pAKT. Furthermore, as *IDH* wild-type status also correlates with increased total and phospho-HSP27, those SPARC-positive tumors wild-type for both *PTEN* and *IDH* may also benefit by targeting HSP27. Thus, any SPARC-positive tumor that is positive for *PTEN*, independent of *IDH* status, may benefit from targeting HSP27.

Our research has focused on identifying therapeutic approaches to inhibit or suppress brain tumor invasion. Based on our signaling model (Figure 1), we propose that tumors that are SPARC+/*PTEN*-null would be more invasively aggressive due to increased HSP27 and its phosphorylated forms, and as a consequence, the patients harboring these tumors would have shorter overall survival. In agreement with a previous publication [35], we found that increasing SPARC expression correlated with decreasing overall patient survival, and additionally progression free survival. However, we found no correlation between intensity of HSP27 expression and overall survival, whether in a *PTEN*-wild-type or *PTEN*-null genetic background. While Mälelä *et al.* [32] found that HSP27 expression was associated with a shorter rate of survival when combining tumors of all grade, they did not see a correlation when looking at each grade separately. As our study is largely comprised of GBMs, we do not have the ability to assess survival over all grades, but our data would agree with the results that no change in survival is attributed to total HSP27 status in grade IV tumors. Also, we found that increasing pAKT was associated with decreasing patient survival, as would be expected, and this was independent of *PTEN* status.

Although we found no correlation between total HSP27 expression and survival, we did find that any expression of S78HSP27 correlated with shorter survival, suggesting that targeting HSP27, and thereby S78HSP27, would enhance patient survival.

Although we found an interesting association between increasing S78HSP27 expression and increased progression-free survival in a *PTEN*-null background, this was not associated with enhanced overall survival. Overall, *PTEN* status does not influence HSP27 and pAKT signaling relative to patient survival.

The rationale for HSP27 as a therapeutic target has been established for several cancer types including breast [36] and prostate cancer [37]. In addition, rationale for the inhibition of AKT signaling through PI3K inhibition is well established [38]. However, a major hurdle for glioma patient treatment is that many drugs that successfully treat other cancer types cannot cross the blood brain barrier to access tumor. Fortunately, the drug buparlisib, a PI3K inhibitor does cross the blood brain barrier [38], as does the p38MAPK inhibitor SB239063, which has been used to treat stroke patients [39, 40]. These drugs provide agents for initial testing our proposed treatment strategy.

## CONCLUSION

In conclusion, we have previously demonstrated that SPARC can promote invasion, which is associated with the upregulation of HSP27 and its phosphorylation at three serine residues. These studies support the contention that HSP27 is a target to suppress SPARC-induced glioma invasion and a target to increase patient survival. We have also shown that *PTEN* can suppress SPARC-induced invasion *in vivo* and signaling *in vitro*. It is clear from this study of human infiltrating astrocytomas that the loss of *PTEN* correlates with increased signaling through AKT and HSP27, supporting our model and the proposed therapeutic targeting of HSP27 in SPARC+/*PTEN*-wild-type tumors or HSP27 and pAKT in SPARC+/*PTEN*-null tumors in the treatment of glioma patients to prevent SPARC-induced tumor invasion.

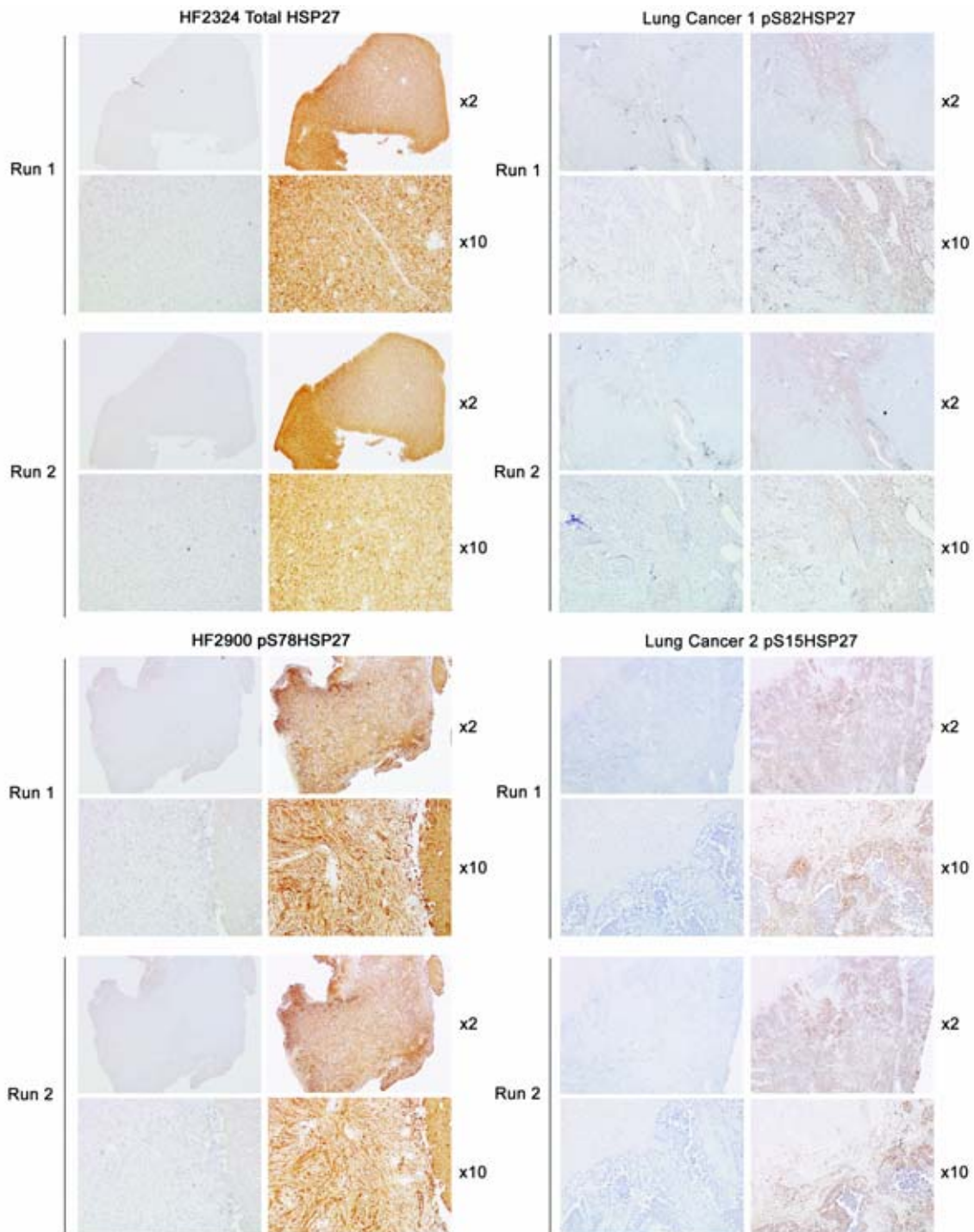
## FUNDING

This National Institutes of Health, National Cancer Institute (5R01CA138401-05 to SAR); Department of Neurosurgery, Henry Ford Hospital, Detroit MI; Spectrum Health System, Grand Rapids, MI.

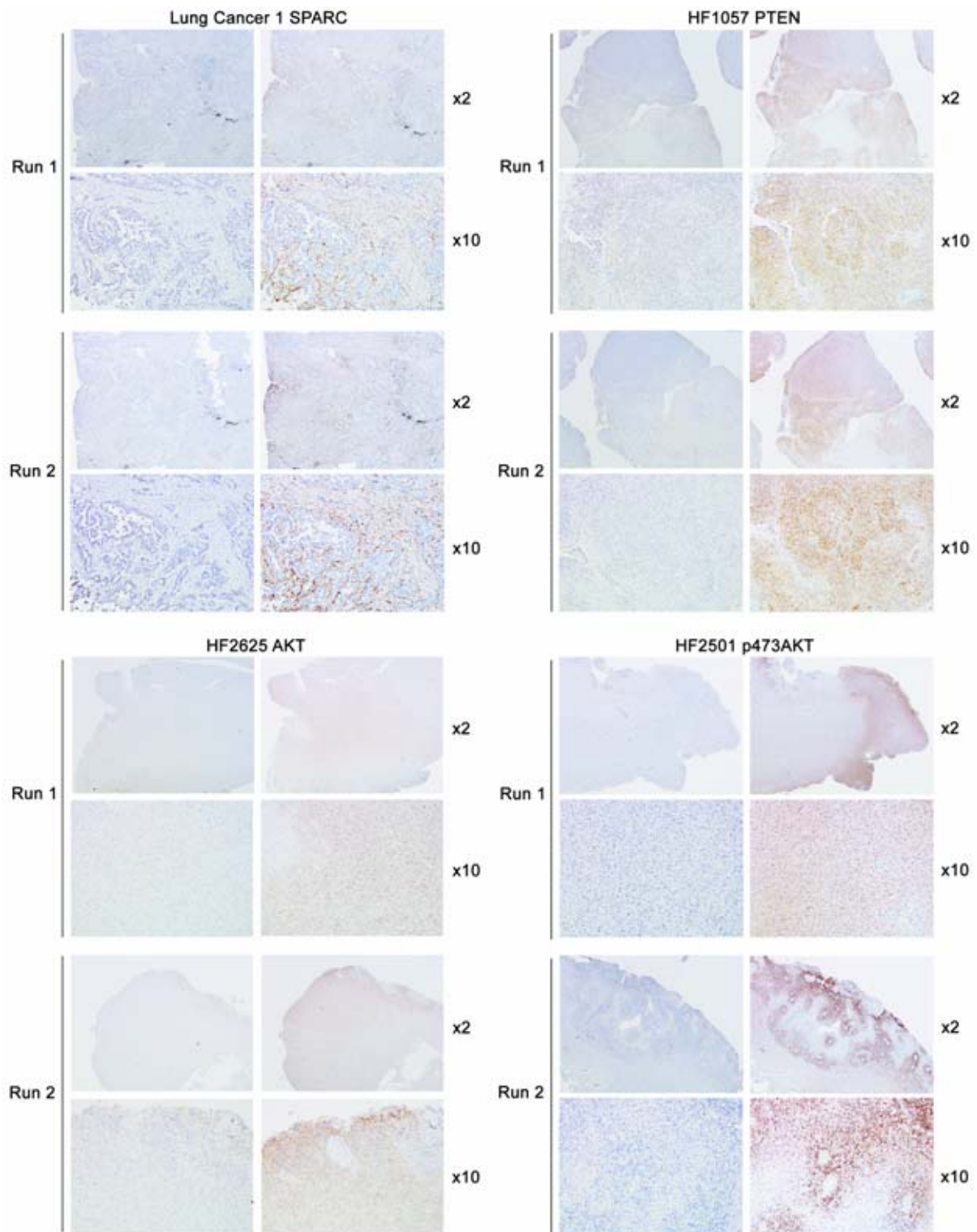
## CONFLICT OF INTEREST STATEMENT

None to declare.

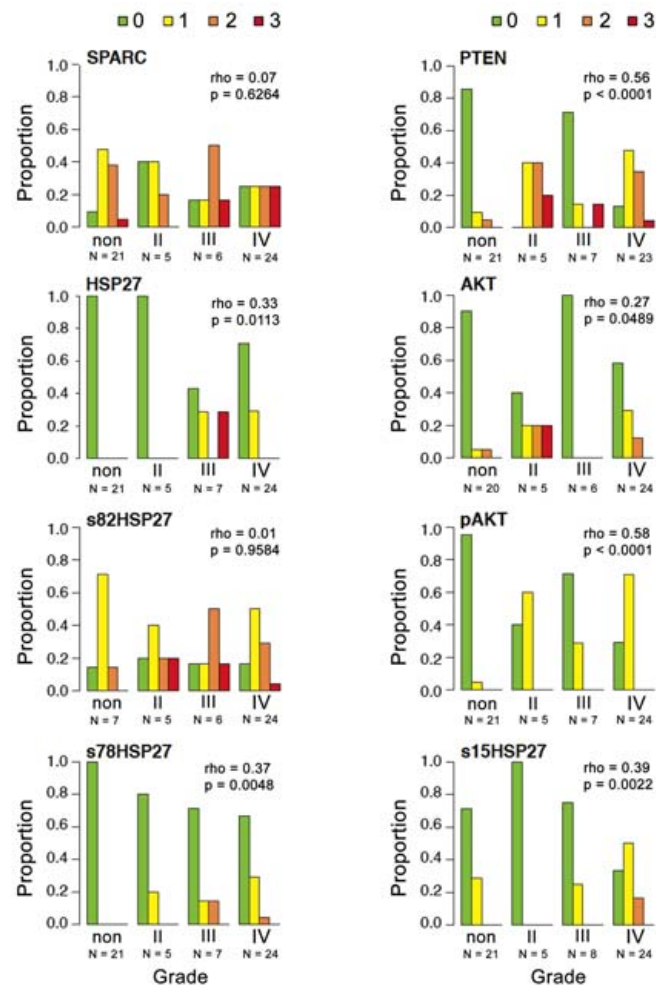
## SUPPLEMENTARY MATERIAL



**Supplementary figure S1.** Immunohistochemistry controls for HSP27, pS82HSP27, pS78HSP27, and pS15HSP27. Control negative and positive tissues used for both immunohistochemistry runs. Control sections were from brain tumor samples used in this study (HF2324 and HF2900) and from primary lung cancer specimens (Lung Cancer 1 and Lung Cancer 2). Magnifications as indicated.



**Supplementary figure S2.** Immunohistochemistry controls for SPARC, AKT, p473AKT, and PTEN. Control negative and positive tissues used for both immunohistochemistry runs. Control sections were from brain tumor samples used in this study (HF1057, HF2625, and HF2501), and from a primary lung cancer specimen (Lung Cancer 1). Magnifications as indicated.

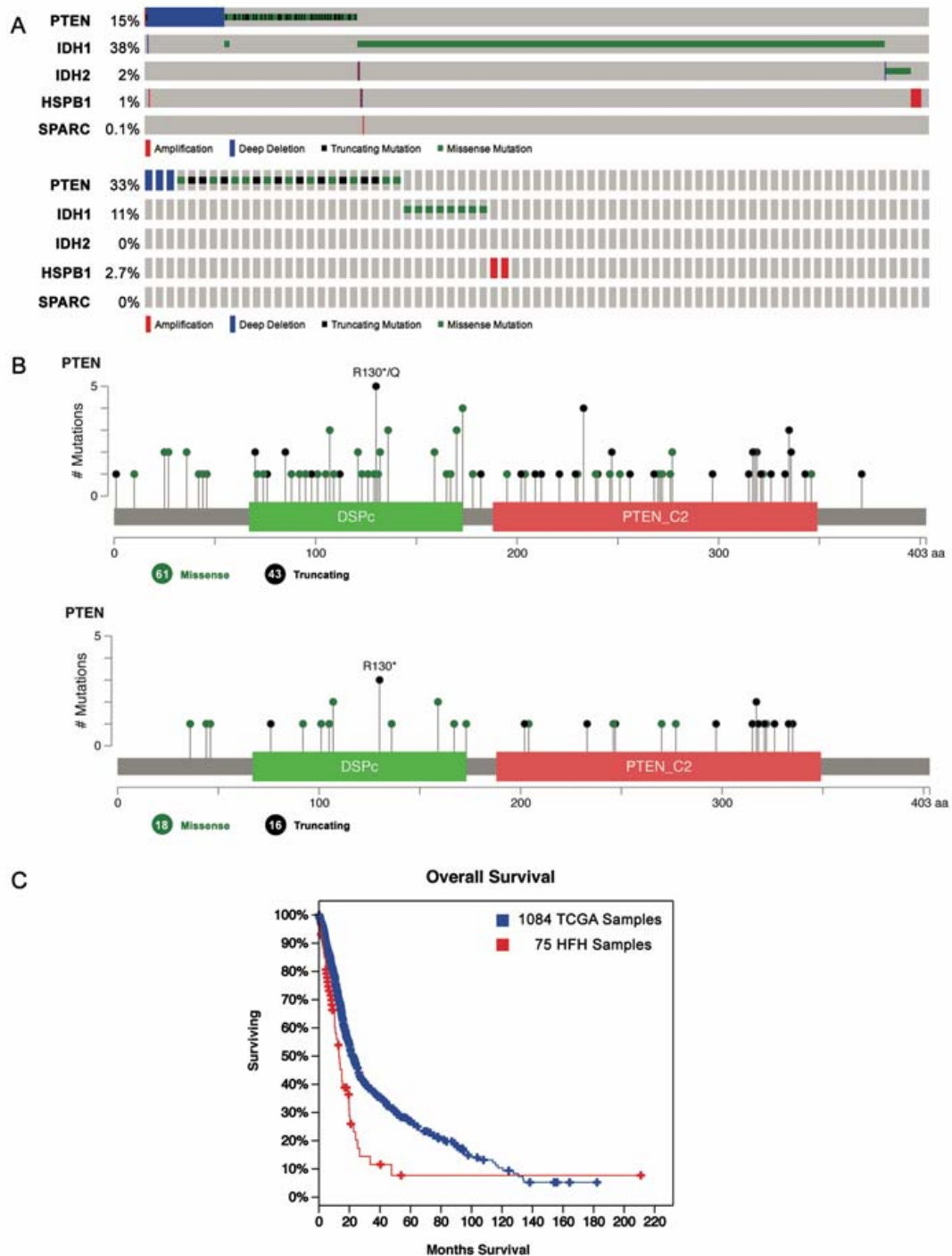


**Supplementary figure S3.** Barplots of staining intensity by grade. The barplots illustrate the proportion of samples per antibody at each staining intensity in the 21 independent normal brain samples compared to that observed in tumor-adjacent normal brain tissue present in the different grades of glioma samples. Levels of expression of HSP27, S78HSP27, S15HSP27, PTEN, AKT, and pAKT are low in independent normal brain tissues, but have increased levels in tumor-adjacent normal brain. SPARC and S82HSP27 are higher in independent normal brain tissues and tumor-adjacent normal brain.

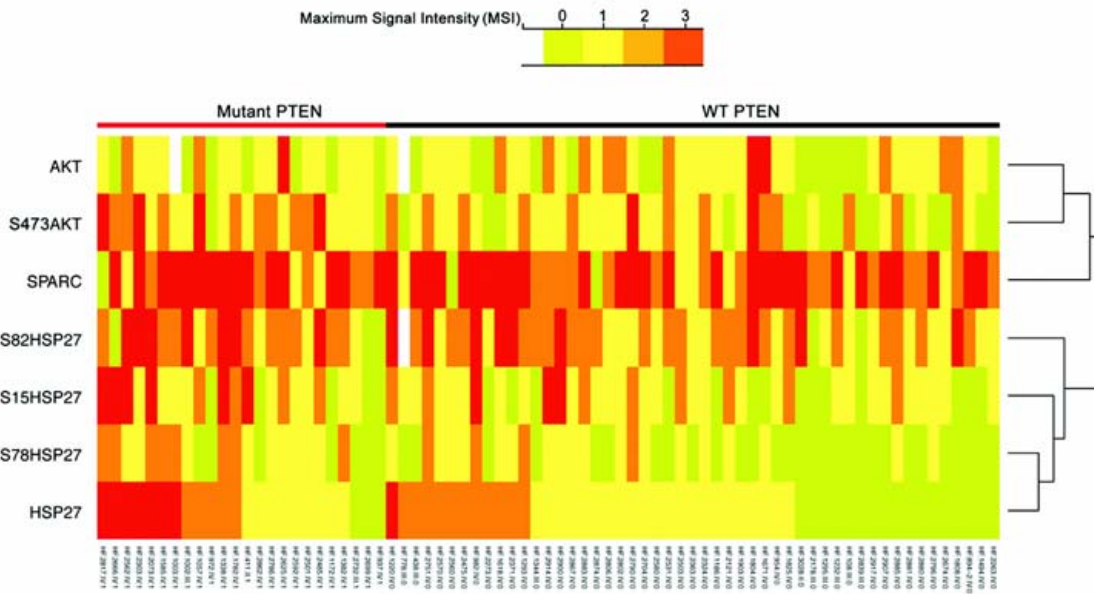
**Supplementary table S1.** Patient profile and sample size for grade, immunohistochemistry, and *PTEN* and *IDH* status.

Tumor Grade	Histology	Immuno	In TCGA	PTEN Status			IDH Status		
				WT	MUT	Total Known	WT	MUT	Total Known
II	A	6	2	1	1	2	1	1	2
III	AA	14	10	8	2	10	8	2	10
IV	GBM	82	75	45	18	63	57	6	63
Subtotal n				54	21		66	9	
Total n		<b>102</b>	<b>87</b>			<b>75</b>			<b>75</b>

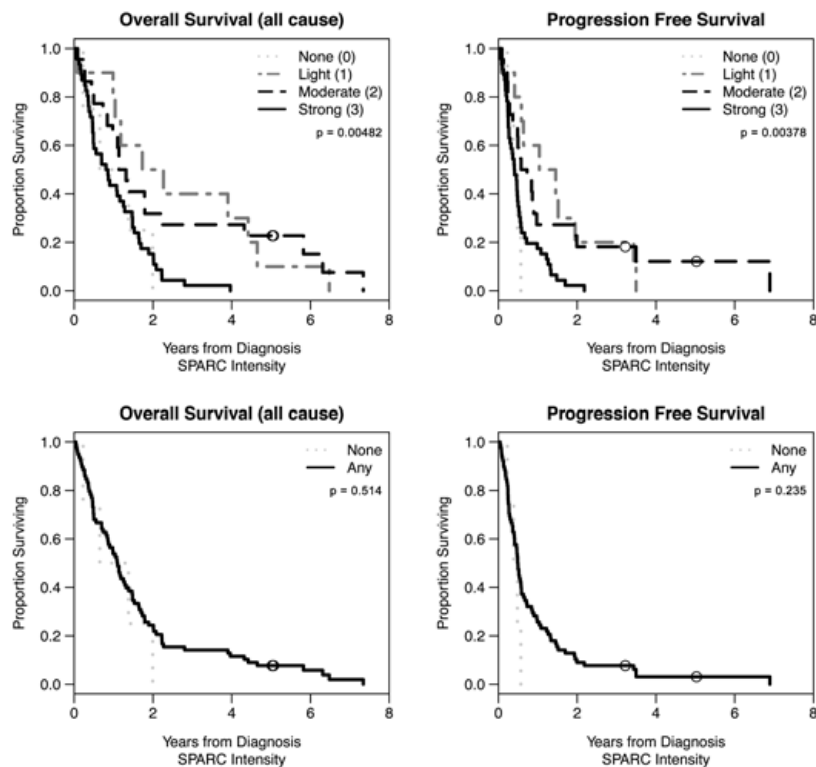
Abbreviations: A, astrocytoma; AA, anaplastic astrocytoma; GBM, glioblastoma; Immuno, immunohistochemistry; W, wild-type; MUT, mutant.



**Supplementary figure S4.** cBioPortal oncoprint of genetic alterations. **A.** Genetic alterations associated with *PTEN*, *IDH1*, *IDH2*, *HSPB1*, and *SPARC* for the 1084 glioma samples in TCGA and those associated with the HFH samples used in this study. (For legibility, the majority of TCGA cases without any alterations are omitted.) The HFH subset is representative of the whole set. **B.** cBioPortal illustration for *PTEN* mutations for the 1084 glioma samples in TCGA and those associated with the HFH samples used in this study. The subset is representative of the whole set. **C.** cBioPortal overall survival curves for the 1084 glioma samples in TCGA and those associated with the HFH samples used in this study. The overall survival for patients in the subset is notably less than that for patients in the whole set. This is due to the high proportion (82%) of grade IV glioma used in this study relative to the proportion (53%) used in the pan-glioma cohort at TCGA.



**Supplementary figure S5.** Heatmaps by *PTEN* status. Heatmaps for HSP27, S82HSP27, S78HSP27, S15HSP27, S473AKT, AKT and SPARC illustrate protein expression patterns based on maximum signal intensity (MSI). Tissues are ordered first by Mutant *PTEN* versus WT (wild-type) *PTEN*, and then by HSP27.



**Supplementary figure S6.** Patient survival relative to SPARC staining. Kaplan-Meier plots showing overall survival and progression-free survival according to the intensity of SPARC staining (top panels) and according to the presence or absence of SPARC staining (bottom panels). Significance is set at  $p \leq 0.05$ .

**Supplementary table S2.** Mutation and copy number (CN) among cases with known *PTEN* status. *PTEN* function loss is assumed for cases in the shaded cells.

	PTEN-WT	PTEN-MUT	Total
Putative CN: -2	3	0	3
Putative CN: -1	44	20	64
Putative CN: 0	7	1	8
Total	54	21	75

**Supplementary table S3.** Immunohistochemistry: antibodies and materials and methods.

Primary Antibody <sup>a</sup>	Retrieval <sup>b</sup>	Block <sup>c</sup> (Biocare)	Dilution <sup>d</sup> (Biocare)	Catalog Number	Company
SPARC**	Citrate	10% NH, A/B	0.5 µl in 10 ml of 0.25% BSA; 60 min	AON5031	Heamatologic Technologies Inc.
HSP27**	Diva	A/B	1:800 in 1:1; 45 min	2402	Cell Signaling
S15HSP27*	Citrate	A/B	1:25 in 1:1; 120 min	SPA-525	Assay Designs/ Enzo Life Sciences
S78HSP27*	Diva	A/B	1:100 in 1:1; 75 min	CS2405	Cell Signaling
S82HSP27*	EDTA	A/B	1:2.5K in 1:1; 60 min	CS2401	Cell Signaling
PTEN **	Citrate	Sniper 7, A/B	1:300 in Renoir Red; 45 min	CM 278 AK, BK	Biocare
AKT***	Citrate	Sniper 7, A/B	1:700; 60 min	CS4685	Cell Signaling
S473 AKT***	Citrate	Sniper 7, A/B	1:700; 60 min	CS4060	Cell Signaling

Immunohistochemistry was performed using a Biocare Nemesis instrument and Biocare reagents unless indicated otherwise.

<sup>a</sup>Primary antibodies: \*polyclonal, \*\*mouse monoclonal, \*\*\*rabbit monoclonal

<sup>b</sup>Retrieval methods:

- Citrate: Sections were incubated for 10 min in 3% hydrogen peroxide, immersed in 10 mM tris buffered saline (TBS; pH 6.0) and boiled for 10 min, and then cooled for 20 min. Sections were rinsed 3 times in phosphate buffered saline (PBS) solution.
- EDTA: Sections were incubated for 10 min in 3% Hydrogen Peroxide, immersed in EDTA Buffer (pH 8.0) and boiled for 10 min, then cooled for 20 min.
- Diva: Slides were immersed in Biocare's Diva Decloaker and retrieved in Biocare's Decloaking Chamber at 80°C for 30 min.

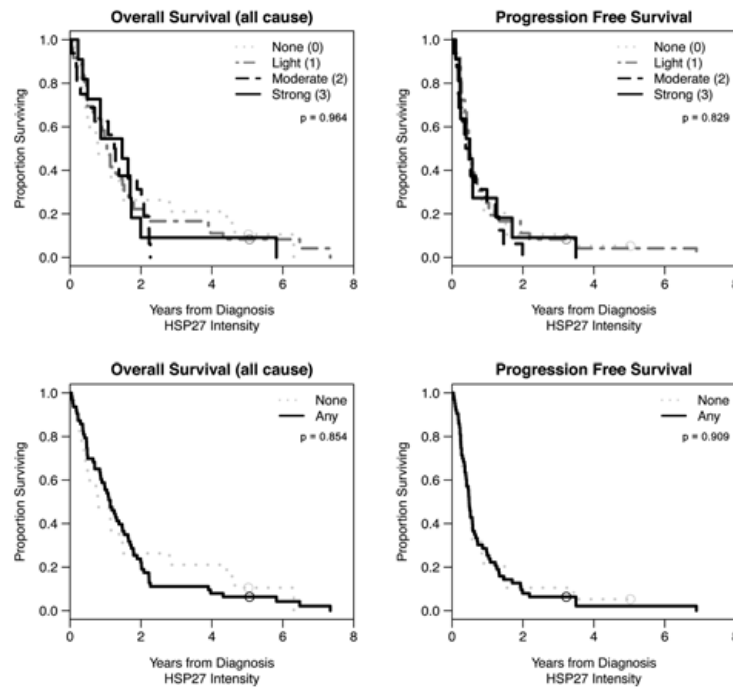
<sup>c</sup>Blocking: For SPARC: NH - normal horse serum

<sup>d</sup>Dilution: Antibodies are diluted in Background Sniper (Biocare) at ratio indicated, except for SPARC and PTEN.

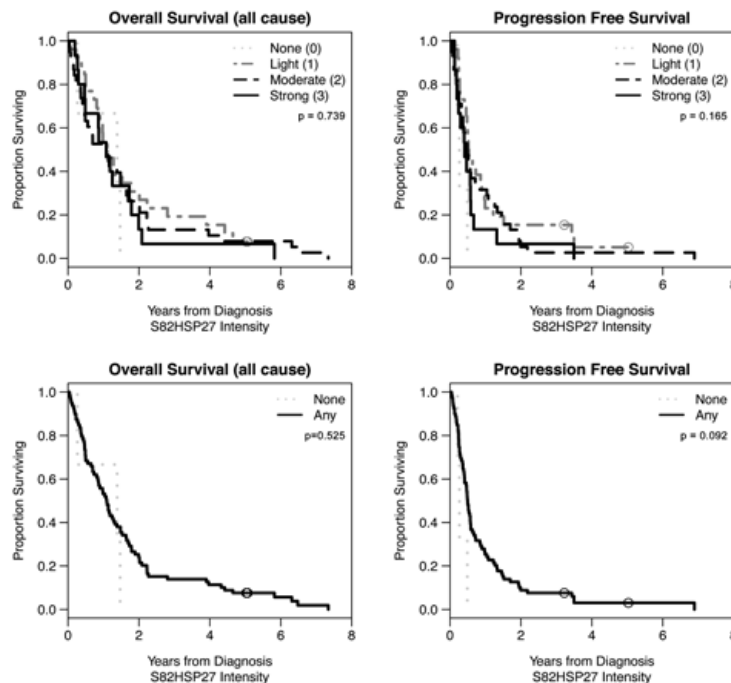
Secondary and Tertiary antibodies: Sections were incubated using Biocare's Universal 4plus Streptavidin HRP Detection Kit, according to the manufacturer's instructions.

Detection: Finally, the sections were washed, reacted with diaminobenzidine (DAB) in 0.1 M Tris buffer (pH 7.6) with 0.03% hydrogen peroxide, followed by rinsing in tap water, counterstaining with hematoxylin, and mounting.

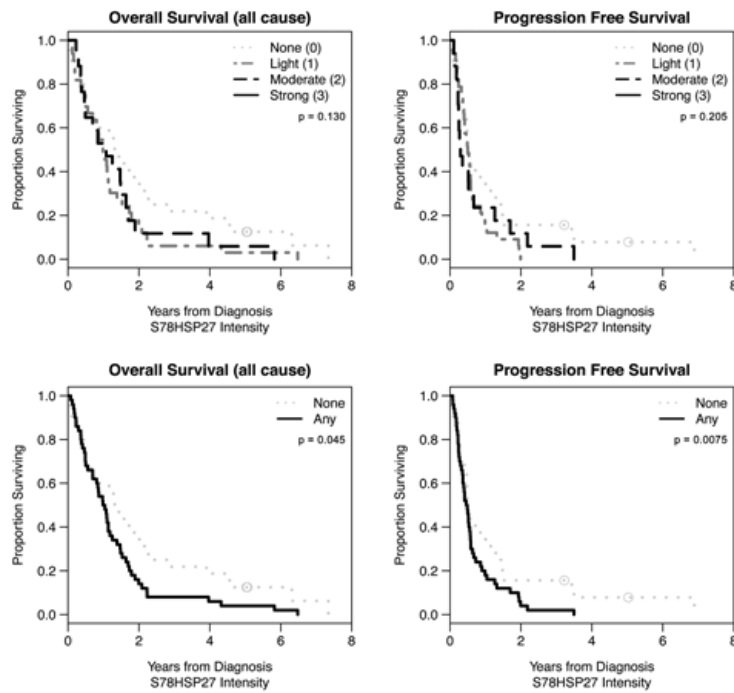
Negative controls were performed omitting the primary antibody and substituting with the Universal Negative Control Serum designed to work with both monoclonal and polyclonal antibodies and with any of Biocare's mouse and/or rabbit streptavidin kits.



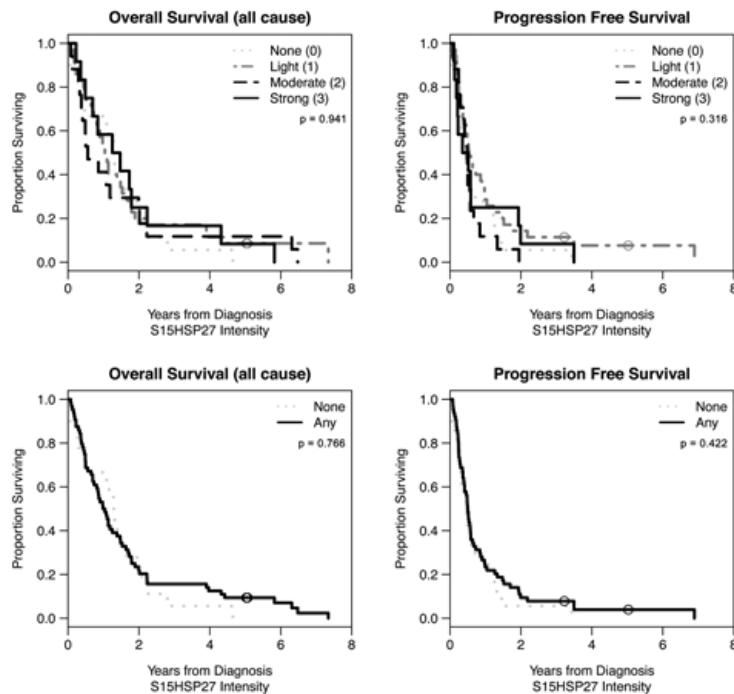
**Supplementary figure S7.** Patient survival relative to HSP27 staining. Kaplan-Meier plots showing overall survival and progression-free survival according to the intensity of HSP27 staining (top panels) and according to the presence or absence of HSP27 staining (bottom panels). Significance is set at  $p \leq 0.05$ .



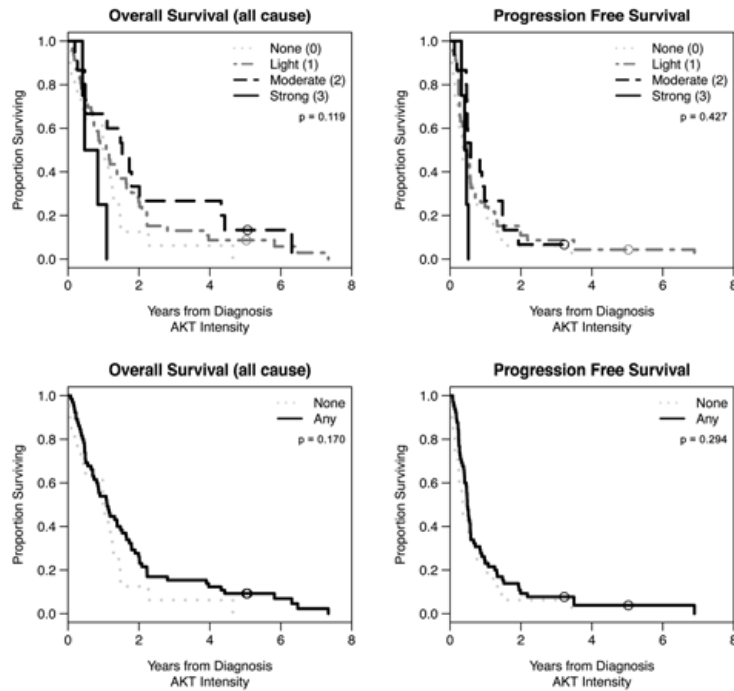
**Supplementary figure S8.** Patient survival relative to S82HSP27 staining. Kaplan-Meier plots showing overall survival and progression-free survival according to the intensity of S82HSP27 staining (top panels) and according to the presence or absence of S82HSP27 staining (bottom panels). Significance is set at  $p \leq 0.05$ .



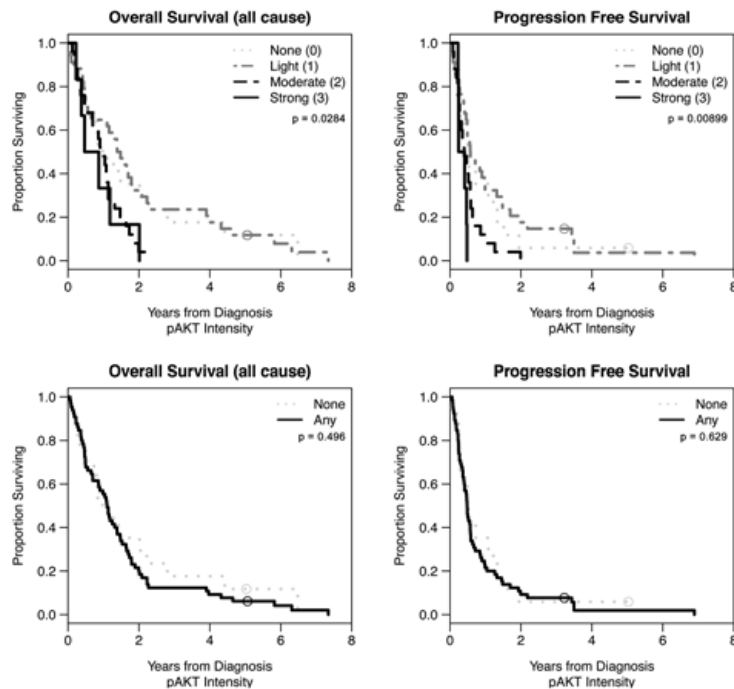
**Supplementary figure S9.** Patient survival relative to S78HSP27 staining. Kaplan-Meier plots showing overall survival and progression free survival according to the intensity of S78HSP27 staining (top panels) and according to the presence or absence of S78HSP27 staining (bottom panels). Significance is set at  $p \leq 0.05$ .



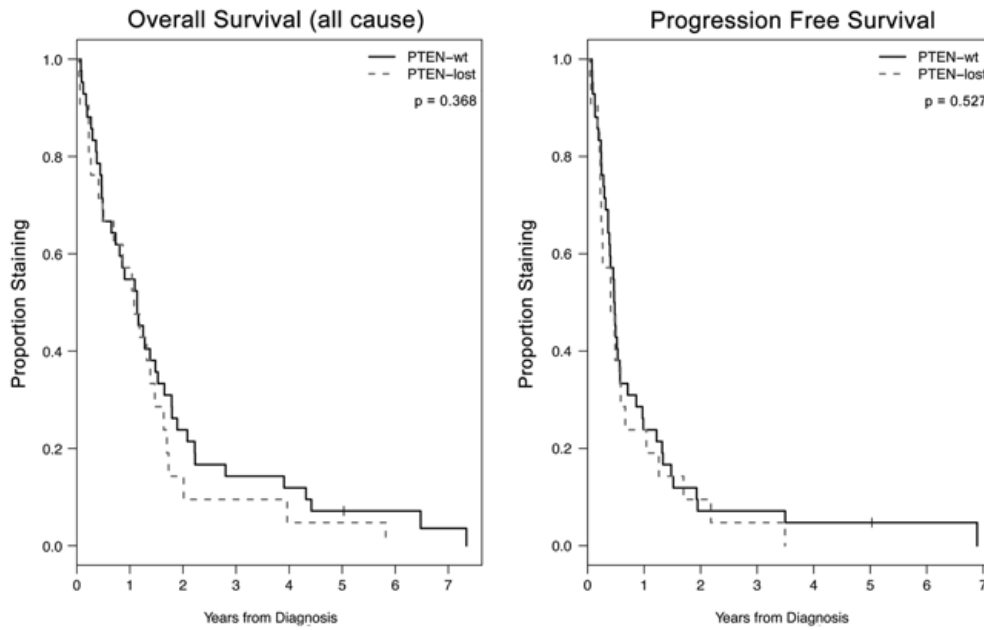
**Supplementary figure S10.** Patient survival relative to S15HSP27 staining. Kaplan-Meier plots showing overall survival and progression-free survival according to the intensity of S15HSP27 staining (top panels) and according to the presence or absence of S15HSP27 staining (bottom panels). Significance is set at  $p \leq 0.05$ .



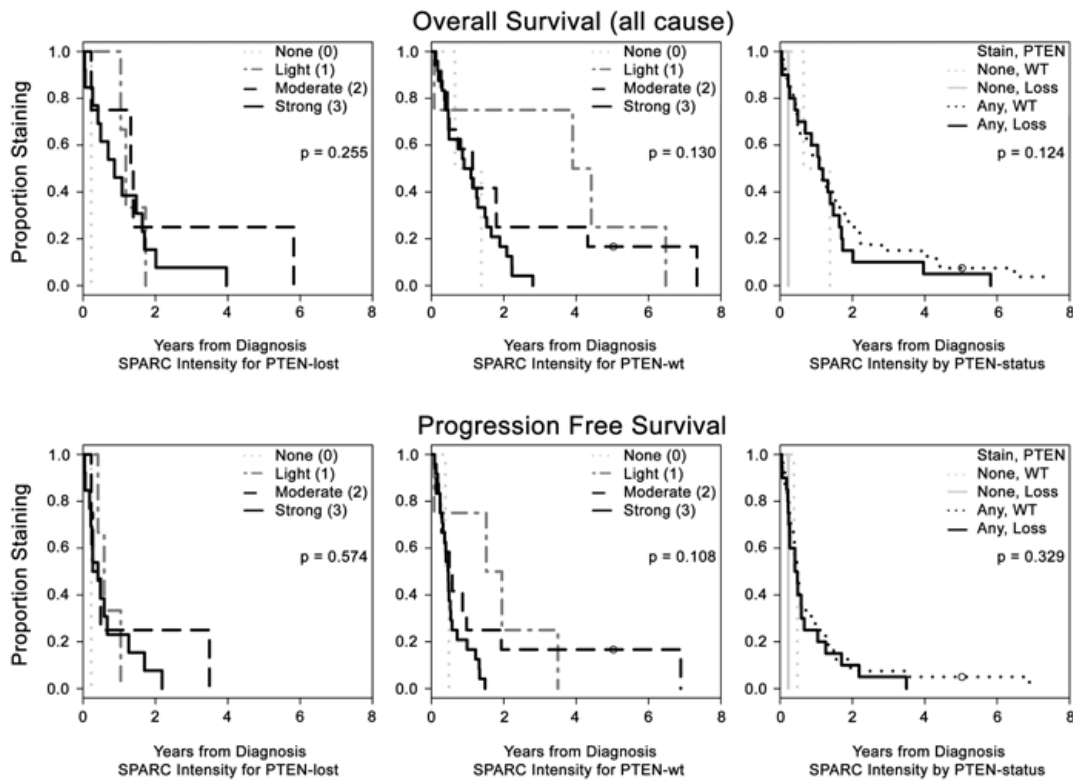
**Supplementary figure S11.** Patient survival relative to AKT staining. Kaplan-Meier plots showing overall survival and progression-free survival according to the intensity of AKT staining (top panels) and according to the presence or absence of AKT staining (bottom panels). Significance is set at  $p \leq 0.05$ .



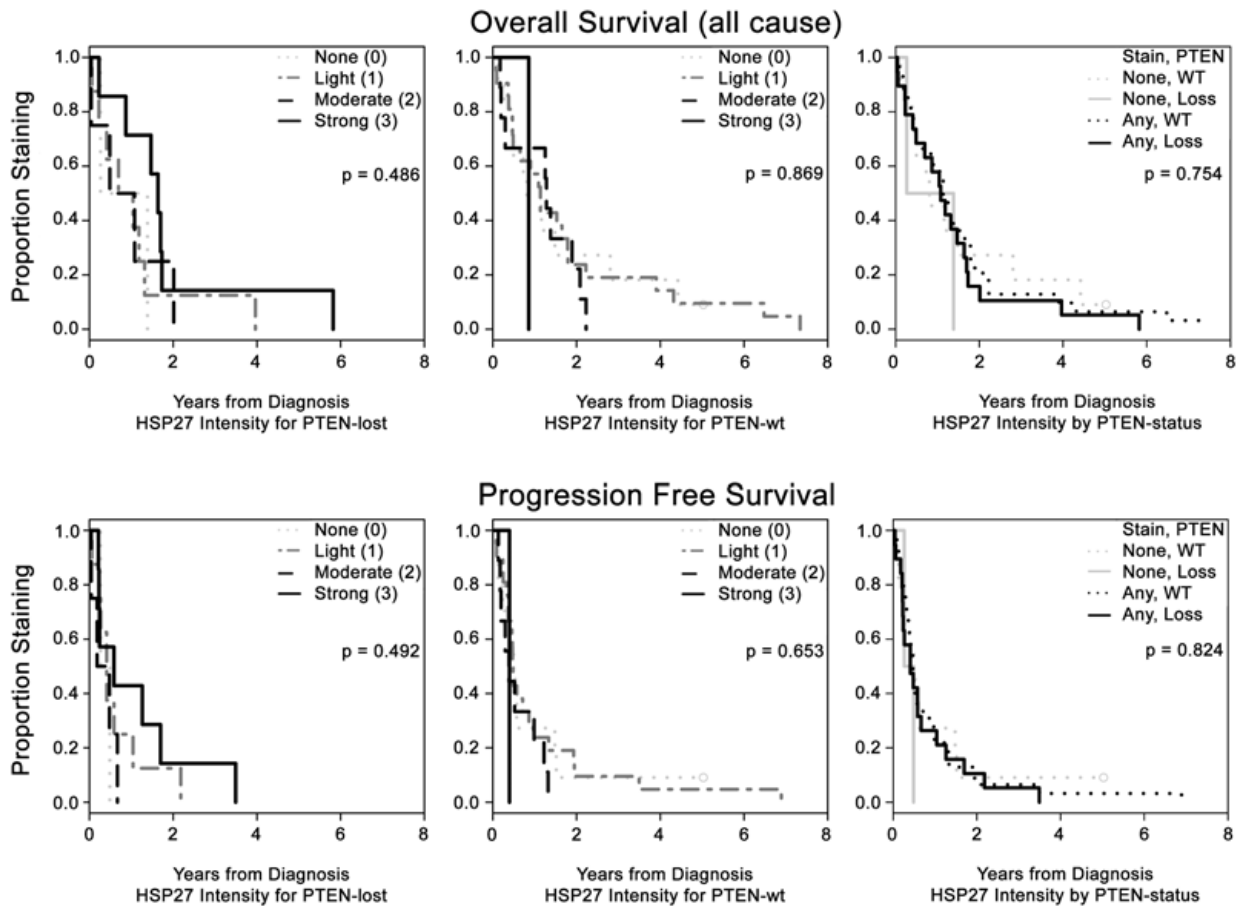
**Supplementary figure S12.** Patient survival relative to pAKT staining. Kaplan-Meier plots showing overall survival and progression-free survival according to the intensity of pAKT staining (top panels) and according to the presence or absence of pAKT staining (bottom panels). Significance is set at  $p \leq 0.05$ .



**Supplementary figure S13.** Patient survival relative to *PTEN* genetic status. Kaplan-Meier plots showing overall survival and progression-free survival according to the presence (*PTEN*-wt) or absence (*PTEN*-lost) of *PTEN*. Significance is set at  $p \leq 0.05$ .



**Supplementary figure S14.** Patient survival relative to SPARC intensity or its presence or absence in *PTEN*-wild-type (*PTEN*-wt) versus *PTEN*-null (*PTEN*-lost) tumors. Kaplan-Meier plots showing overall survival (top panels) and progression-free survival (bottom panels). Significance is set at  $p \leq 0.05$ .



**Supplementary figure S15.** Patient survival relative to HSP27 intensity or its presence or absence in *PTEN*-wild-type (*PTEN*-wt) versus *PTEN*-null (*PTEN*-lost) tumors. Kaplan-Meier plots showing overall survival (top panels) and progression-free survival (bottom panels). Significance is set at  $p \leq 0.05$ .

**Supplementary table S4.** *PTEN* genetic status by intensity of *PTEN* expression.

	0	1	2	3
PTEN WT	4	10	10	4
PTEN MUT	1	4	5	4

**Supplementary table S5.** *PTEN* genetic status by grade.

	II	III	IV
PTEN WT	1 (50%)	8 (80%)	45 (71%)
PTEN MUT	1 (50%)	2 (20%)	18 (29%)

**Supplementary table S6.** *PTEN* genetic status by *IDH* genetic status.

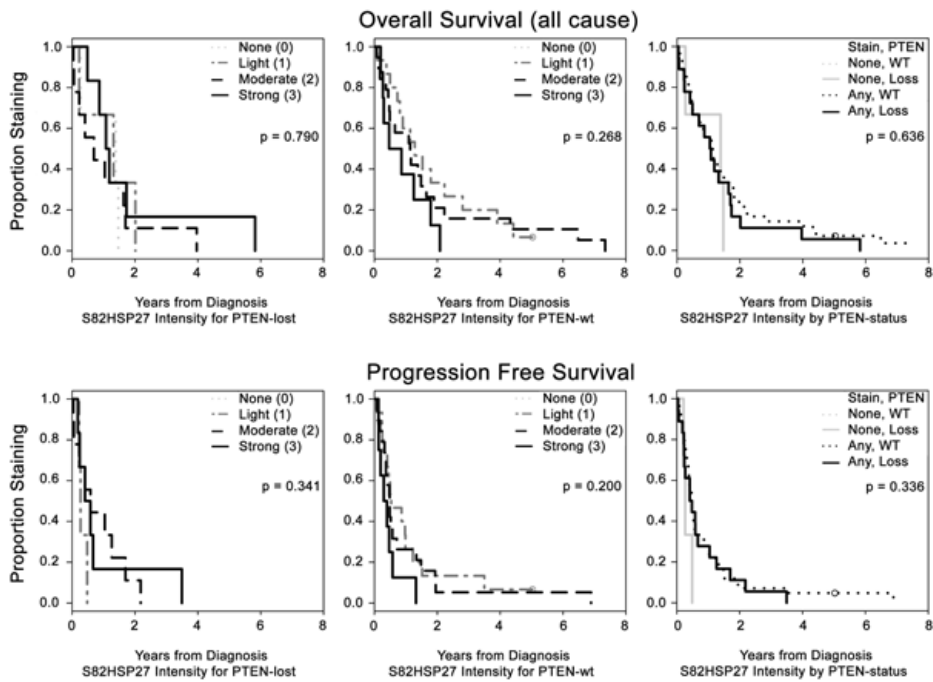
	IDH WT	IDH MUT
PTEN WT	45 (68%)	9 (100%)
PTEN MUT	21 (32%)	0 (0%)

**Supplementary table S7.** *IDH* genetic status by grade.

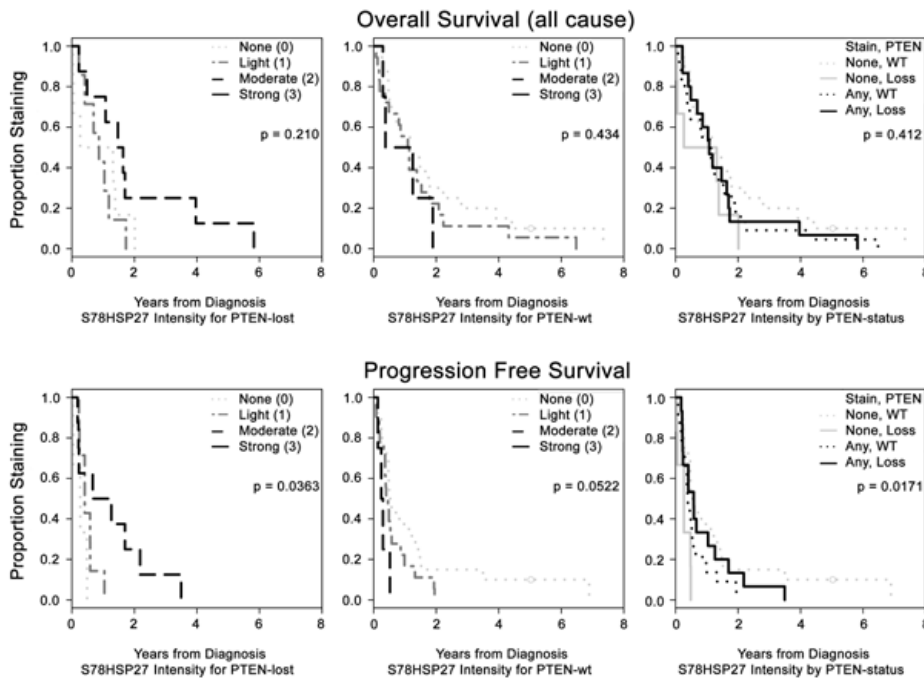
	II	III	IV
IDH WT	1 (50%)	8 (80%)	57 (90%)
IDH MUT	1 (50%)	2 (20%)	6 (10%)

**Supplementary table S8.** *IDH1* genetic status by intensity of SPARC expression.

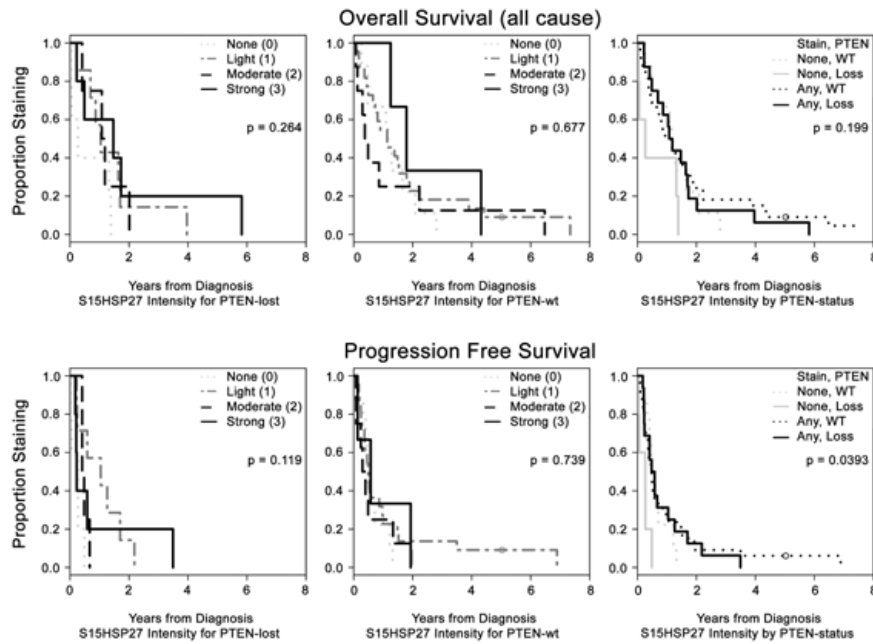
	0	1	2	3
IDH WT	3	9	15	39
IDH MUT	0	0	5	4



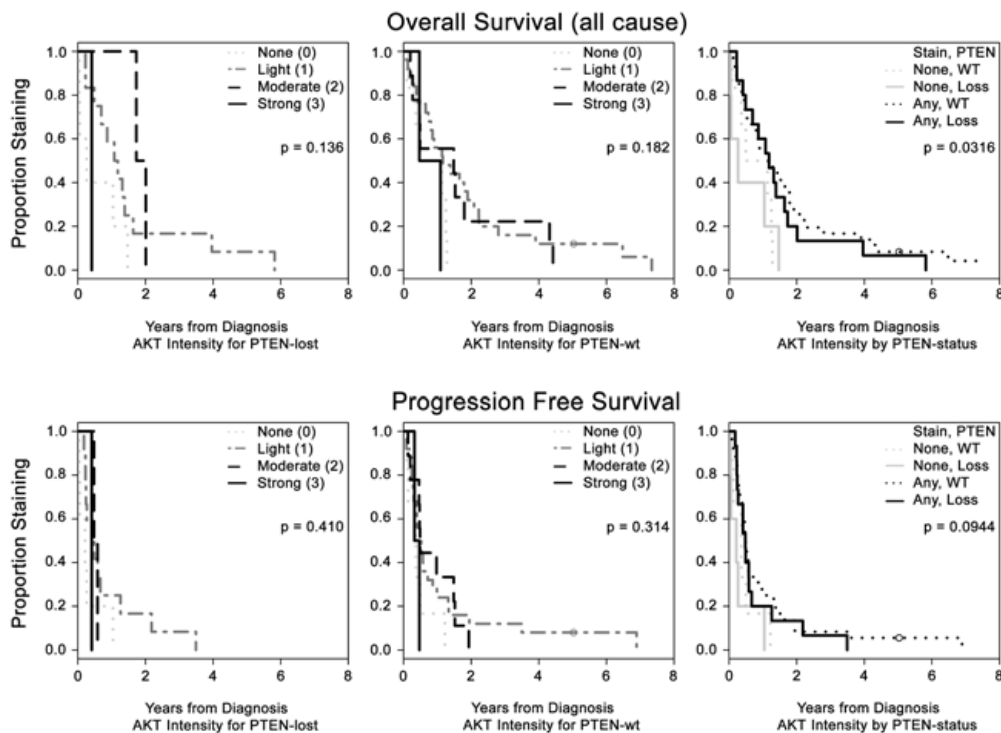
**Supplementary figure S16.** Patient survival relative to S82HSP27 intensity or its presence or absence in *PTEN* -wild-type (*PTEN*-wt) versus *PTEN*-null (*PTEN*-lost) tumors. Kaplan-Meier plots showing overall survival (top panels) and progression-free survival (bottom panels). Significance is set at  $p \leq 0.05$ .



**Supplementary figure S17.** Patient survival relative to S78HSP27 intensity or its presence or absence in *PTEN*-wild-type (*PTEN*-wt) versus *PTEN*-null (*PTEN*-lost) tumors. Kaplan-Meier plots showing overall survival (top panels) and progression-free survival (bottom panels). Significance is set at  $p \leq 0.05$ .



**Supplementary figure S18.** Patient survival relative to S15HSP27 intensity or its presence or absence in *PTEN*-wild-type (*PTEN*-wt) versus *PTEN*-null (*PTEN*-lost) tumors. Kaplan-Meier plots showing overall survival (top panels) and progression-free survival (bottom panels). Significance is set at  $p \leq 0.05$ .



**Supplementary figure S19.** Patient survival relative to AKT intensity or its presence or absence in *PTEN*-wild-type (*PTEN*-wt) versus *PTEN*-null (*PTEN*-lost) tumors. Kaplan-Meier plots showing overall survival (top panels) and progression-free survival (bottom panels). Significance is set at  $p \leq 0.05$ .

**Supplementary database S1.** Normal tissue immunohistochemistry and tissue features.

HF#	Normal Brain & Associated Pathologies	HSP27	S82HSP27	S78HSP27	S15HSP27	AKT	S473AKT	SPARC	Cerebral Cortex	SPARC+ cells
HF0317	Hematoma	0	1	0	0	0	0	1	Cortex present and negative	Bergmann glia
HF0319	Ependymoma	0	1	0	0	0	0	2	Cortex present but positive	Reactive astrocytes (RA) and neurons
HF0347	Anaplastic squamous cell carcinoma	0		0	1	2	1	1	Cortex present but positive	Bergmann glia, neurons and astrocytes
HF0350	AA to GBM	0		0	0	0	0	1	Cortex present and negative	Bergmann glia
HF0351	GBM	0		0	0	0	0	1	Cortex present and negative	Bergmann glia
HF0352	Pituitary adenocarcinoma	0		0	1	0	0	1	Cortex present and negative	Bergmann glia
HF0353	Pituitary adenoma	0		0	0	0	0	1	Cortex present and negative	Bergmann glia
HF0354	Metastatic adenocarcinoma	0		0	1	0	0	1	Cortex present and negative	Bergmann glia
HF0355	GBM	0		0	0	0	0	0	Cortex present and negative	
HF0356	Alzheimer II Gliosis	0		0	1		0	0	Cortex present and negative	
HF0358	Metastatic	0		0	1	1	0	2	Cortex present but positive	neurons, astrocytes and oligodendrocytes in white matter
HF0593	Mild gliosis including neurons	0	0	0	0	0	0	2	Cortex and hippocampus present but positive	Bergmann glia and neurons
HF0594	Mild gliosis including neurons	0	1	0	1	0	0	2	Cortex present but positive	Bergmann glia and neurons
HF0616	Extensive focal rarefaction	0	1	0	0	0	0	2	No cortex; ependymal lining-deep grey or hypothalamic	RA
HF0638	Mild gliosis including neurons	0	1	0	0	0	0	2	No cortex	RA
HF0721	No pathological changes	0		0	0	0	0	1	No cortex; ependymal and deep grey matter	RA
HF0739	No pathological changes	0		0	0	0	0	1	Cortex present but positive	RA

Supplementary database S1 continued..

H0F744	Seizures, oligodendroglioma, gliosis	0	2	0	0	0	0	0	0	2	Cortex and hippocampus present but positive	Bergman glia and neurons
HF0753	No pathological changes	0		0	0	0	0	0	0	1	Cortex and hippocampus present but positive	Bergman glia and neurons
HF0764	Gliosis	0		0	0	0	0	0	0	3	Cortex and hippocampus present but positive	RA
HF0786	Hematoma	0		0	0	0	0	0	0	2	Cortex present but positive	RA, white matter gliosis

Abbreviations: HF#, Henry Ford Hospital Tumor Bank ID number. Empty cell, lost section.

**Supplementary database S2. Tumor immunohistochemistry and TCGA data. (Part I)**

Tumor Samples			Immunohistochemistry											
HF#	Histology	Grade	HSP27			S82HSP27			S78HSP27					
			Intensity TC	% TC	Intensity NB	Intensity TC	% TC	Intensity NB	Intensity TC	% TC	Intensity NB			
HF2263	GBM	IV	0	0	0	1	5	0	0	0	0	0	0	
HF1003	GBM	IV	3	3		2	1		2	2		2		
HF1382	GBM	IV	1	1	0	2	3	1	2	1	1	0	0	
HF1293	GBM	IV	2	3		2	2		2	2		2		
HF1494	GBM	IV	0	0	0	1	5	0	0	0	0	0	0	
HF1782	GBM	IV	2	2		3	5		2	3		2		
HF2371	GBM	IV	2	5		3	5		1	5		1		
HF1825	GBM	IV	1	1	0	2	2	1	0	0	1	0	1	
HF1220	GBM	IV	3	5		3	5		1	1		1		
HF1618	GBM	IV	2	2		3	2		1	2		1		
HF0894	GBM	IV	0	0		2	5		0	0		0		
HF0937	GBM	IV	0	0		0	0		0	0		0		
HF0954	GBM	IV	1	1	0	1	1	0	0	0	0	0	0	
HF1338	GBM	IV	2	1		3	2		2	1		2		
HF1585	GBM	IV	3	3	1	2	3	1	2	2	1	2	0	
HF1671	GBM	IV	1	1	0	2	3	1	1	1	1	1	0	
HF1804	GBM	IV	1	1		3	1		0	0		0		
HF1808	GBM	IV	0	0	0	3	2	2	0	0	2	0	0	
HF1903	GBM	IV	1	1		2	5		0	0		0		
HF2073	GBM	IV	3	2		3	2		2	1		2		
HF2121	GBM	IV	1	1		2	2		1	1		1		
HF2273	GBM	IV	2	5		1	5		0	0		0		
HF2303	GBM	IV	3	3	0	3	3	1	1	1	1	2	0	
HF0972	GBM	IV	2	5		2	5		0	0		0		
HF0982	GBM	IV	2	2	0	3	5	2	2	2	2	2	0	
HF1057	GBM	IV	2	3		1	3		0	0		0		
HF1172	GBM	IV	1	1		2	1		0	0		0		
HF1186	GBM	IV	1	1		2	3		0	0		0		
HF2324	GBM	IV	1	5		1	2		1	1		1		
HF2475	GBM	IV	2	5		2	5		1	1		1		
HF2485	GBM	IV	1	1		3	5		1	1		1		
HF2363	GBM	IV	1	1		1	3		0	0		0		
HF2501	GBM	IV	1	1		1	5		1	1		1		

Supplementary database S2 (Part I) continued..

Immunohistochemistry																			
S15HSP27					SPARC					PTEN					p473AKT				
Intensity TC	% TC	Intensity NB	Intensity TC	% TC	Intensity NB	Intensity TC	% TC	Intensity NB	Intensity TC	% TC	Intensity NB	Intensity TC	% TC	Intensity NB	Intensity TC	% TC	Intensity NB	Intensity TC	% TC
1	5	1	2	5	0	2	5	0	2	5	2	5	0	2	0	0	2	0	0
1	1		3	5		1	5		1	1		1		1	1	1		1	
1	3	1	3	5	1	3	5	1	3	4	1	4	1	3	1	1	1	1	0
1	2		3	5		2	5		2	3		3		2	1	1		2	
0	0	0	3	5	0	3	5	0	3	2	1	2	0	3	0	0	1	0	0
2	5		3	4		3	4		3	4		4		3	2	2		2	
0	0		3	5		2	5		2	3		3		2	1	1		1	
2	5	1	3	4	0	3	4	0	3	2	1	2	0	3	0	0	1	0	1
2	1		3	5		3	5		3	3		3		3	2	3		2	
1	2		3	4		3	4		3	2		2		2	0	0		0	
0	0		3	5		3	5		3	3		3		3	1	1		1	
0	0		3	5		3	5		3	0		0		0	0	0		0	
1	2	0	3	5	1	3	5	1	3	4	1	4	1	3	2	1	1	2	1
3	2		3	3		3	3		3	3		3		2	1	1		1	
1	1	0	3	4	2	3	4	2	3	2	2	3	2	3	2	2	2	2	0
0	0	0	3	4	2	3	4	2	3	2	2	4	0	3	2	4	0	4	0
0	0		3	4		3	4		3	4		2		2	3	1		1	
0	0	0	2	2	3	2	2	3	2	2	2	2	2	2	2	2	2	2	0
1	5		2	5		2	5		2	1		2		1	1	1		1	
3	2		2	5		2	5		2	3		5		3	1	1		1	
2	1		1	2		1	2		1	2		2		2	0	0		0	
0	0		3	5		3	5		3	1		5		1	0	0		0	
1	2	0	3	5	2	3	5	2	3	3	0	5	0	3	3	2	1	2	1
0	0		3	5		3	5		3	1		2		1	0	0		0	
3	5	1	3	4	3	3	4	3	3	4	3	4	3	3	1	1	1	1	0
2	3		3	3		2	3		2	2		2		2	3	2		2	
0	0		3	3		3	3		3	3		3		1	1	1		1	
0	0		3	5		3	5		3	3		3		2	1	1		1	
1	1		2	5		2	5		2	2		3		2	2	2		2	
1	1		3	5		3	5		3	1		5		1	2	3		3	
2	5		1	3		1	3		1	2		5		2	3	5		5	
1	5		1	2		1	2		1	1		5		1	1	2		2	
1	5		2	2		2	2		2	2		5		2	2	2		2	

Supplementary database S2 (Part I) continued..

Immunohistochemistry				TCGA Data													
AKT				PTEN						IDH				Survival	Vital status	Age at Diagnosis	Gender
Intensity TC	% TC	Intensity NB	Whole. exome	Whole. genome	PTEN. copies	PTEN. mut	1 = mutation	0 = loss	IDH. status	Months	1 = dead.						
0	0	0	Yes	No	-1	NaN	0	0	WT	6.14	1	84	female				
			Yes	Yes	-1	T277I	1	1	WT	20.37	1	67	male				
1	1	0	Yes	Yes	-1	T319*	1	1	WT	47.57	1	63	female				
1	1		Yes	Yes	-1	NaN	0	0	Mutant	22.70	1	66	male				
1	2	0	Yes	No	-1	NaN	0	0	Mutant	33.64	1	30	male				
1	2		Yes	No	-2	NaN	0	1	WT	12.94	1	54	male				
1	1		Yes	No	-1	NaN	0	0	WT	25.33	1	49	male				
1	2	0	Yes	No	-1	NaN	0	0	WT	26.68	1	63	female				
1	2		Yes	No	-1	NaN	0	0	WT	10.28	1	62	male				
2	4		Yes	Yes	-1	NaN	0	0	WT	2.33	1	53	female				
1	3		Yes	No	-1	NaN	0	0	WT	13.93	1	54	male				
0	0		Yes	Yes	-1	Y76*	1	1	WT	3.19	1	63	female				
1	2	0	Yes	No	-1	NaN	0	0	WT	10.81	1	73	male				
1	1		Yes	No	-1	T167S	1	1	WT	5.85	1	51	male				
1	4	0	Yes	No	-1	A328*	1	1	WT	19.65	1	59	female				
3	4	0	Yes	Yes	-1	NaN	0	0	WT	13.11	1	65	male				
3	1		Yes	No	-1	NaN	0	0	WT	4.47	1	72	female				
2	4	1	Yes	No	-1	NaN	0	0	WT	3.22	1	54	male				
1	1		Yes	No	0	NaN	0	0	Mutant	53.95	0	38	male				
1	1		Yes	No	-1	G36E	1	1	WT	40.35	0	63	male				
1	1		Yes	Yes	-1	NaN	0	0	WT	36.99	0	54	male				
0	0		Yes	No	-1	NaN	0	0	WT	15.41	1	55	male				
1	2	1	Yes	Yes	-1	D92E	1	1	WT	10.42	1	62	male				
0	0		Yes	No	-1	R335*	1	1	WT	0.53	1	55	female				
0	0	0	Yes	Yes	-1	NaN	0	0	WT	15.01	1	66	male				
2	5		Yes	No	-1	D107H	1	1	WT	24.15	1	61	female				
0	0		Yes	No	-2	NaN	0	1	WT	0.72	1	67	male				
1	1		Yes	Yes	-1	NaN	0	0	Mutant	19.81	1	31	male				
1	5		Yes	No	-1	NaN	0	0	WT	13.63	1	75	female				
1	5		Yes	No	-1	NaN	0	0	WT	2.10	1	73	female				
1	5		Yes	Yes	-2	NaN	0	1	WT	9.40	0	53	male				
1	5		Yes	Yes	-1	NaN	0	0	WT	19.55	0	66	male				
1	1		Yes	No	-1	D297if s*10	1	1	WT	2.69	1	50	male				

Supplementary database S2 (Part II)

Tumor Samples			Immunohistochemistry											
HF#	Histology	Grade	HSP27			S82HSP27			S78HSP27					
			Intensity TC	% TC	Intensity NB	Intensity TC	% TC	Intensity NB	Intensity TC	% TC	Intensity NB			
HF2503	GBM	IV	1	1		2	3		1	1		1	1	
HF2531	GBM	IV	1	1	1	2	5		0	0	1	0	0	0
HF2560	GBM	IV	2	3		2	5		1	1		1	2	
HF2562	GBM	IV	3	2		3	2		1	1		1	1	
HF2570	GBM	IV	2	1		1	1		1	1		1	1	
HF2580	GBM	IV	1	2		1	2		0	0		0	0	
HF2592	GBM	IV	1	1	1	2	3		3	1		1	1	1
HF2625	GBM	IV	1	1	1	2	2		2	1		1	1	1
HF2666	GBM	IV	3	5		0	0		2	2		2	2	
HF2674	GBM	IV	0	0		1	2		0	0		0	0	
HF2699	GBM	IV	0	0		0	0		0	0		0	0	
HF2704	GBM	IV	1	1	0	2	5		2	1		1	1	1
HF2751	GBM	IV	2	1	0	3	4		2	2		2	2	2
HF2786	GBM	IV	1	1		2	2		1	1		1	1	
HF2790	GBM	IV	1	1		1	3		2	3		2	3	
HF2796	GBM	IV	0	0		1	2		1	1		1	1	
HF2802	GBM	IV	1	1		1	1		1	1		1	1	
HF2806	GBM	IV	1	1		1	4		0	0		0	0	
HF2817	GBM	IV	3	1		2	3		2	2		2	2	
HF2862	GBM	IV	1	4	0	1	2		0	1		0	0	0
HF2874	GBM	IV	1	1		2	4		0	0		0	0	
HF2880	GBM	IV	0	0	0	2	2		1	1		0	0	0
HF2881	GBM	IV	0	0		1	5		0	0		0	0	
HF2883	GBM	IV	1	1		2	3		1	2		1	2	
HF2885	GBM	IV	0	0	0	2	4		1	1		1	1	0
HF2867	GBM	IV	1	2		2	3		1	2		1	2	
HF2900	GBM	IV	1	2		3	5		1	1		1	1	
HF2907	GBM	IV	0	0	0	2	3		0	0		0	0	0
HF2914	GBM	IV	1	1		2	5		1	1		1	1	
HF2917	GBM	IV	0	0		1	5		0	0		0	0	
HF2732	AA	III	0	0		1	1		0	0		0	0	
HF2839	AA	III	0	0		0	0		0	0		0	0	
HF0108	AA	III	0	0		1	5		0	0		0	0	
HF1002	AA	III	2	3		3	5		1	2		1	2	
HF1232	AA	III	0	0	1	2	2		0	0	1	0	0	1

Supplementary database S2 (Part II) continued..

Immunohistochemistry												
S15HSP27			SPARC			PTEN			p473AKT			
Intensity TC	% TC	Intensity NB	Intensity TC	% TC	Intensity NB	Intensity TC	% TC	Intensity NB	Intensity TC	% TC	Intensity NB	Intensity TC
2	2		1	4		3	5		1	1		1
0	0	1	3	5	3	1	3	2	2	2		2
1	2		0	0		2	4		1	1		1
3	2		1	1		3	5		2	1		1
1	1		3	5		2	2		1	2		1
1	2		2	5		0	0		1	1		1
1	2	1	1	1	0	1	3	2	2	2		2
2	5	2	3	1	2	2	3	1	1	1		1
3	5		3	5		2	3		2	2		2
1	1		1	2		1	1		0	0		0
0	0		2	5		0	0		1	2		2
1	1	1	3	4	0	1	1	1	1	1		1
2	3	1	3	5	1	2	2	1	2	2		2
1	1		3	5		1	2		2	2		2
2	2		3	5		1	1		3	4		4
1	1		3	5		1	1		0	0		0
1	1		3	5		2	4		1	1		1
1	1		2	5		0	0		1	1		1
3	1		0	0		2	4		3	2		2
0	0	0	2	5	2	3	5	1	2	5		5
1	1		0	0		3	5		1	1		1
1	5	1	2	5	1	1	3	3	1	1		1
1	5		2	5		1	5		0	0		0
2	3		3	5		1	2		1	2		2
2	4	2	3	5	3	3	5	2	2	5		5
1	2		2	5		0	0		2	2		2
3	5		2	5		2	5		1	2		2
1	1	0	3	5	1	2	5	2	1	1		1
3	5		2	5		3	5		1	1		1
1	5		2	5		2	5		0	0		0
2	3		3	5		1	2		1	2		2
2	4		3	5		3	5		1	2		2
1	2		2	5		0	0		2	2		2
3	5		2	5		2	5		1	2		2
1	1	0	3	5	1	2	5	2	1	1		1
3	5		2	5		3	5		1	1		1
1	5		2	5		2	5		0	0		0
1	0		2	5		2	5		1	1		1
0	0		3	5		2	3		0	0		0
1	5		1	5		2	5		2	5		5
1	1	1	3	5	2	3	5	1	1	1		1
1	2		3	5		1	5		0	0		0

Supplementary database S2 (Part II) continued..

Immunohistochemistry				TCGA Data														
AKT				PTEN						IDH				Survival		Vital status	Age at Diagnosis	Gender
Intensity TC	% TC	Intensity NB	Whole. exome	Whole. genome	PTEN. copies	PTEN.mut	1 = mutation	0 = loss	IDH. status	Months	1 = dead.	Months	1 = dead.	Age at Diagnosis	Gender			
1	4		Yes	No	-1	NaN	0	0	WT	0.92	1	0.92	1	43	male			
2	3	1	Yes	Yes	-1	NaN	0	0	WT	6.70	0	6.70	0	78	male			
1	1		Yes	Yes	-1	NaN	0	0	WT	5.85	0	5.85	0	50	male			
2	2		Yes	No	-1	R173H	1	1	WT	5.42	0	5.42	0	30	male			
1	2		Yes	No	-1	NaN	0	0	WT	20.93	0	20.93	0	79	female			
0	0		Yes	Yes	-1	NaN	0	0	WT	1.08	1	1.08	1	76	male			
0	0	0	Yes	No	-1	R130*	1	1	WT	12.48	1	12.48	1	75	female			
3	5	2	Yes	No	-1	R159S	1	1	WT	4.93	1	4.93	1	83	male			
0	0		Yes	No	-1	T319*	1	1	WT	9.27	0	9.27	0	53	female			
2	5		Yes	No	0	NaN	0	0	WT	8.51	0	8.51	0	72	female			
1	5		Yes	No	-1	I101T	1	1	WT	6.80	0	6.80	0	59	male			
0	0	0	Yes	No	-1	NaN	0	0	WT	4.37	1	4.37	1	65	male			
1	3	0	Yes	No	-1	NaN	0	0	WT	3.55	1	3.55	1	72	female			
1	1		Yes	Yes	-1	R130*	1	1	WT	8.35	1	8.35	1	51	male			
1	2		Yes	No	-1	NaN	0	0	WT	4.53	1	4.53	1	78	female			
1	4		Yes	No	-1	NaN	0	0	WT	8.81	0	8.81	0	67	male			
2	5		Yes	No	-1	NaN	0	0	WT	8.97	0	8.97	0	61	male			
2	1		Yes	Yes	-1	NaN	0	0	WT	8.54	0	8.54	0	60	male			
1	1		Yes	No	-1	P204L	1	1	WT	2.73	1	2.73	1	75	female			
1	3	0	Yes	No	0	R233*	1	1	WT	6.14	0	6.14	0	45	female			
1	5		Yes	No	-1	NaN	0	0	WT	4.57	0	4.57	0	63	male			
1	3	1	Yes	No	-1	NaN	0	0	WT	5.22	1	5.22	1	64	female			
1	5		Yes	No	0	NaN	0	0	Mutant	7.79	0	7.79	0	49	female			
2	5		Yes	No	-1	NaN	0	0	WT	5.39	1	5.39	1	58	male			
1	3	0	Yes	No	0	NaN	0	0	WT	1.48	1	1.48	1	44	female			
0	0		Yes	No	-1	NaN	0	0	WT	8.31	0	8.31	0	64	male			
1	1		Yes	No	-1	NaN	0	0	WT	12.85	0	12.85	0	65	male			
2	4	2	Yes	No	-1	NaN	0	0	WT	1.54	0	1.54	0	58	female			
2	5		Yes	No	-1	NaN	0	0	WT	4.76	0	4.76	0	76	male			
1	5		Yes	No	0	NaN	0	0	Mutant	4.96	0	4.96	0	60	male			
1	2		Yes	Yes	-1	T319Nfs*6	1	1	WT	18.00	0	18.00	0	34	female			
0	0		Yes	Yes	-1	NaN	0	0	WT	8.44	0	8.44	0	57	female			
0	0		Yes	Yes	0	NaN	0	0	WT	211.03	0	211.03	0	35	female			
0	0		Yes	Yes	-1	D107Y	1	1	WT	7.03	1	7.03	1	52	male			
0	0	0	Yes	Yes	-1	NaN	0	0	WT	19.88	1	19.88	1	51	female			

Supplementary database S2 (Part III)

Tumor Samples			Immunohistochemistry											
HF#	Histology	Grade	HSP27			S82HSP27			S78HSP27					
			Intensity TC	% TC	Intensity NB	Intensity TC	% TC	Intensity NB	Intensity TC	% TC	Intensity NB			
HF0438	AA	III	2	4		2	5		0	0		0	0	
HF1295	AA	III	0	0	1	1	5	2	0	0	2	0	0	0
HF1344	AA	III	1	2		2	3		0	0		0	0	
HF0778	AA	III	2	5	0				0	0		0	0	0
HF2178	AA	III	0	0	3				2	4		0	0	0
HF0411	A	II	1	1		2	3		0	0		1	2	
HF3028	OA	II	0	0	0				3	5		0	0	0
HF2637	A	II	2	4	0				2	4		1	1	0
HF2865	A	II	0	0	0				0	0		0	0	0
HF2882	A	II	0	0	0				3	5		0	0	1
HF3014	A	II	0	0	0				3	5		0	0	0
HF2498	AA	III	0	0	0				2	5		0	0	0
HF2499	AA	III	2	5	0				2	5		1	3	0
HF2585	AA	III	3	5		2	5		2	5		1	5	
HF2773	AA	III	0	0	3				0	0		0	0	2
HF1058	GBM	IV	1	1		2	5		2	5		2	1	
HF1490	GBM	IV	0	0		2	2		0	0		0	0	
HF1540	GBM	IV	1	1		1	1		2	4		2	1	
HF1958	GBM	IV	1	1		2	4		0	0		0	0	
HF2238	GBM	IV	2	2		2	2		0	0		0	0	
HF2316	GBM	IV	2	1		2	5		1	3		1	3	
HF2323	GBM	IV	1	1		1	5		1	1		1	1	
HF2385	GBM	IV	0	0	0				2	4		0	0	0
HF2566	GBM	IV	3	3		3	5		1	1		1	1	
HF2587	GBM	IV	1	1	1				1	1		1	1	1
HF2701	GBM	IV	3	2	1				1	1		1	1	1
HF2810	GBM	IV	1	1	1				1	2		0	0	0
HF2814	GBM	IV	0	0					1	1		0	0	
HF2829	GBM	IV	0	0					1	1		1	1	
HF2998	GBM	IV	3	5		2	5		2	5		2	5	
HF3001	GBM	IV	0	0		2	5		2	5		1	1	
HF3018	GBM	IV	2	1	0				2	5		2	5	1
HF3019	GBM	IV	0	0		2	5		2	5		1	1	
HF3026	GBM	IV	1	1		1	2		1	2		2	1	

Supplementary database S2 (Part III) continued..

Immunohistochemistry														
S15HSP27				SPARC				PTEN				p473AKT		
Intensity TC	% TC	Intensity NB	Intensity TC	% TC	Intensity NB	Intensity TC	% TC	Intensity NB	Intensity TC	% TC	Intensity NB	Intensity TC	% TC	Intensity NB
1	5		3	5		2	5		1			1	4	
0	0	0	2	2	2	2	2	0	0		0	0	0	0
0	0	0	2	5		1	3		1			1	1	
1	5	0	1	5	1	0	0	0	0		0	0	0	0
0	0	0	2	5	3	2	5	3	1		3	1	1	1
3	5		3	5		2	5		2			1	2	
0	0	0	3	5	2	1	5	1	0		1	0	0	1
2	1	0	2	5	0	2	5	2	2		2	1	1	0
0	0	0	3	5	1	0	0	2	0		2	0	0	1
0	0	0	3	5	0	2	5	1	2		1	1	3	0
0	0	0	2	5	1	1	5	3	2		3	2	5	1
0	0	0	3	5	0	1	5	0	1		0	0	0	0
1	5	0	1	3	0	3	5	0	3		0	2	5	0
2	5		3	5		3	5		3			0	0	
0	0	1	3	5	2	3	5	0	3		0	1	1	1
0	0		3	5		2	5		2			0	0	
2	3		3	4		1	3		1			0	0	
3	3		2	3		1	3		1			0	0	
0	0		3	4		2	3		2			0	0	
0	0		1	1		2	3		2			1	1	
3	5		2	4		3	2		3			2	2	
1	1		2	5		2	5		2			0	0	
2	5	2	2	4	1	2	2	2	1		2	1	1	1
2	2		0	0		2	5		2			2	2	
1	5	1	1	5	0	1	5	1	1		1	2	2	1
2	1	1	3	5	3	1	1	0	2		0	2	2	1
1	5	1	2	5	3	1	1	1	1		1	1	5	1
0	0		1	1		2	3		2			1	1	
1	1		2	3		1	5		1			1	5	
3	5		3	5		3	5		3			2	2	
1	2		3	5		2	5		2			1	2	
3	5	2	3	5	2	3	5	1	3		1	2	3	1
2	2		3	5		2	5		2			1	5	
1	1		3	5		3	2		2			1	1	

Supplementary database S2 (Part III) continued..

Immunohistochemistry				TCGA Data										
AKT				PTEN						IDH	Survival	Vital. status	Age at Diagnosis	Gender
Intensity TC	% TC	Intensity NB	Whole. exome	Whole. genome	PTEN .copies	PTEN. mut	1 = mutation	0 = loss	IDH. status	Months	1 = dead.			
0	0	0	Yes	Yes	-1	NaN	0	0	WT	11.47	1	60	female	
0	0	0	Yes	Yes	-1	NaN	0	0	Mutant	14.98	1	58	female	
0	0	0	Yes	Yes	-1	NaN	0	0	WT	8.84	1	59	male	
0	0	0	Yes	Yes	-1	NaN	0	0	WT	7.95	1	69	male	
0	0	0	Yes	No	-1	NaN	0	0	Mutant	18.92	1	38	female	
0	0	0	Yes	Yes	-1	C105Y	1	1	WT	10.35	1	45	female	
0	0	0	Yes	No	0	NaN	0	0	Mutant	16.95	0	29	female	
0	0	1												
0	0	2												
1	2	0												
2	5	3												
0	0	0												
0	0	0												
1	3													
2	1	0												
0	0													
1	4													
3	5													
1	2													
0	0													
1	2													
0	0													
2	5	2												
1	2													
0	0	0												
2	2	1												
2	5	1												
0	0													
2	5													
1	5													
1	5													
1	4	1												
1	2													
1	2													

Abbreviations: TCGA, The Cancer Genome Atlas; HFH, Samples not submitted to TCGA; HF#, HFH sample ID number; TC, tumor cells; NB, normal brain; NaN, no mutations detected.

## REFERENCES

1. Louis, D. N., Ohgaki, H., Wiestler, O. D., Cavenee, W. K., Burger, P. C., Jouvet, A., Scheithauer, B. W. and Kleihues, P. 2007, *Acta Neuropathol.*, 114, 97.
2. Gao, J., Aksoy, B. A., Dogrusoz, U., Dresdner, G., Gross, B., Sumer, S. O., Sun, Y., Jacobsen, A., Sinha, R., Larsson, E., Cerami, E., Sander, C. and Schultz, N. 2013, *Sci. Signal.*, 6, p11.
3. Cerami, E., Gao, J., Dogrusoz, U., Gross, B. E., Sumer, S. O., Aksoy, B. A., Jacobsen, A., Byrne, C. J., Heuer, M. L., Larsson, E., Antipin, Y., Reva, B., Goldberg, A. P., Sander, C. and Schultz, N. 2012, *Cancer Discov.*, 2, 401.
4. Ceccarelli, M., Barthel, F. P., Malta, T. M., Sabedot, T. S., Salama, S. R., Murray, B. A., Morozova, O., Newton, Y., Radenbaugh, A., Pagnotta, S. M., Anjum, S., Wang, J., Manyam, G., Zoppioli, P., Ling, S., Rao, A. A., Grifford, M., Cherniack, A. D., Zhang, H., Poisson, L., Carloti, C. G. Jr., Tirapelli, D. P., Rao, A., Mikkelsen, T., Lau, C. C., Yung, W. K., Rabadan, R., Huse, J., Brat, D. J., Lehman, N. L., Barnholtz-Sloan, J. S., Zheng, S., Hess, K., Rao, G., Meyerson, M., Beroukhim, R., Cooper, L., Akbani, R., Wrensch, M., Haussler, D., Aldape, K. D., Laird, P. W. and Gutmann, D. H. 2016, *Cell*, 164, 550.
5. Louis, D. N., Perry, A., Reifenberger, G., von Deimling, A., Figarella-Branger, D., Cavenee, W. K., Ohgaki, H., Wiestler, O. D., Kleihues, P. and Ellison, D. W. 2016, *Acta Neuropathol.*, 131, 803.
6. Stupp, R., Mason, W. P., van den Bent, M. J., Weller, M., Fisher, B., Taphoorn, M. J., Belanger, K., Brandes, A. A., Marosi, C., Bogdahn, U., Curschmann, J., Janzer, R. C., Ludwin, S. K., Gorlia, T., Allgeier, A., Lacombe, D., Cairncross, J. G., Eisenhauer, E. and Mirimanoff, R. O.; European Organisation for Research and Treatment of Cancer Brain Tumor and Radiotherapy Groups; National Cancer Institute of Canada Clinical Trials Group. 2005, *N. Engl. J. Med.*, 352, 987.
7. Hegi, M. E., Diserens, A. C., Gorlia, T., Hamou, M. F., de Tribolet, N., Weller, M., Kros, J. M., Hainfellner, J. A., Mason, W., Mariani, L., Bromberg, J. E., Hau, P., Mirimanoff, R. O., Cairncross, J. G., Janzer, R. C. and Stupp, R. 2005, *N. Engl. J. Med.*, 352, 997.
8. Wick, W., Wick, A., Schulz, J. B., Dichgans, J., Rodemann, H. P. and Weller, M. 2002, *Cancer Res.*, 62, 1915.
9. de Groot, J. F., Fuller, G., Kumar, A. J., Piao, Y., Eterovic, K., Ji, Y. and Conrad, C. A. 2010, *Neuro Oncol.*, 12, 233.
10. Sage, E. H., Johnson, C. and Bornstein, P. 1984, *J. Biol. Chem.*, 259, 3993.
11. Termine, J. D., Kleinman, H. K., Whitson, S. W., Conn, K. M., McGarvey, M. L. and Martin, G. R. 1981, *Cell*, 26, 99.
12. Mann, K., Deutzmann, R., Paulsson, M. and Timpl, R. 1987, *FEBS Lett.*, 218, 167.
13. Rempel, S. A., Golembieski, W. A., Ge, S., Lemke, N., Elisevich, K., Mikkelsen, T. and Gutiérrez, J. A. 1998, *J. Neuropathol. Exp. Neurol.*, 57, 1112.
14. Parsons, D. W., Jones, S., Zhang, X., Lin, J. C., Leary, R. J., Angenendt, P., Mankoo, P., Carter, H., Siu, I. M., Gallia, G. L., Olivi, A., McLendon, R., Rasheed, B. A., Keir, S., Nikolskaya, T., Nikolsky, Y., Busam, D. A., Tekleab, H., Diaz, L. A. Jr., Hartigan, J., Smith, D. R., Strausberg, R. L., Marie, S. K., Shinjo, S. M., Yan, H., Riggins, G. J., Bigner, D. D., Karchin, R., Papadopoulos, N., Parmigiani, G., Vogelstein, B., Velculescu, V. E. and Kinzler, K. W. 2008, *Science*, 321, 1807.
15. Golembieski, W. A., Ge, S., Nelson, K., Mikkelsen, T. and Rempel, S. A. 1999, *Int. J. Dev. Neurosci.*, 17, 463.
16. Schultz, C., Lemke, N., Ge, S., Golembieski, W. A. and Rempel, S. A. 2002, *Cancer Res.*, 62, 6270.
17. Rich, J. N., Shi, Q., Hjelmeland, M., Cummings, T. J., Kuan, C.T., Bigner, D. D., Counter, C. M. and Wang, X. F. 2003, *J. Biol. Chem.*, 278, 15951.
18. Seno, T., Harada, H., Kohno, S., Teraoka, M., Inoue, A. and Ohnishi, T. 2009, *Int. J. Oncol.*, 34, 707.
19. Golembieski, W. A., Thomas, S. L., Schultz, C. R., Yunker, C. K., McClung, H. M., Lemke, N., Cazacu, S., Barker, T., Sage, E. H., Brodie, C. and Rempel, S. A. 2008, *Glia*, 56, 1061.
20. Alam, R., Schultz, C. R., Golembieski, W. A., Poisson, L. M. and Rempel, S. A. 2013, *Neuro Oncol.*, 15, 451.

21. Zheng, C., Lin, Z., Zhao, Z. J., Yang, Y., Niu, H. and Shen, X. 2006, *J. Biol. Chem.*, 281, 37215.
22. Manning, B. D. and Cantley, L. C. 2007, *Cell*, 129, 1261.
23. Wiencke, J. K., Zheng, S., Jelluma, N., Tihan, T., Vandenberg, S., Tamgüney, T., Baumber, R., Parsons, R., Lamborn, K. R., Berger, M. S., Wrench, M. R., Haas-Kogan, D. A. and Stokoe, D. 2007, *Neuro Oncol.*, 9, 271.
24. Endersby, R. and Baker, S. J. 2008, *Oncogene*, 2, 5416.
25. Thomas, S. L., Alam, R., Lemke, N., Schultz, L. R., Gutiérrez, J. A. and Rempel, S. A. 2010, *Neuro Oncol.*, 12, 941.
26. Schultz, C. R., Golembieski, W. A., King, D. A., Brown, S. L., Brodie, C. and Rempel, S. A. 2012, *Mol. Cancer*, 11, 20.
27. Capper, D., Mittelbronn, M., Goepfert, B., Meyermann, R. and Schittenhelm, J. 2010, *Neuropathol. Appl. Neurobiol.*, 36, 183.
28. Khalid, H., Tsutsumi, K., Yamashita, H., Kishikawa, M., Yasunaga, A. and Shibata, S. 1995, *Cell Mol. Neurobiol.*, 15, 257.
29. Hitotsumatsu, T., Iwaki, T., Fukui, M. and Tateishi, J. 1996, *Cancer*, 77, 352.
30. Strik, H. M., Weller, M., Frank, B., Hermisson, M., Deininger, M. H., Dichgans, J. and Meyermann, R. 2000, *Anticancer Res.*, 20, 4457.
31. Hermisson, M., Strik, H., Rieger, J., Dichgans, J., Meyermann, R. and Weller, M. 2000, *Neurology*, 54, 1357.
32. Mäkelä, K. S., Haapasalo, J. A., Ilvesaro, J. M., Parkkila, S., Paavonen, T. and Haapasalo, H. K. 2014, *Histol. Histopathol.*, 29, 1161.
33. Alexiou, G. A., Karamoutsios, A., Lallas, G., Ragos, V., Goussia, A., Kyritsis, A. P., Voulgaris, S. and Vartholomatos, G. 2014, *Turk. Neurosurg.*, 24, 745.
34. Kostenko, S. and Moens, U. 2009, *Cell Mol. Life Sci.*, 66, 3289.
35. Rich, J. N., Hans, C., Jones, B., Iversen, E. S., McLendon, R. E., Rasheed, B. K., Dobra, A., Dressman, H. K., Bigner, D. D., Nevins, J. R. and West, M. 2005, *Cancer Res.*, 65, 4051.
36. Kim, L. S. and Kim, J. H. 2011, *J. Breast Cancer*, 14, 167.
37. Chi, K. N., Yu, E. Y., Jacobs, C., Bazov, J., Kollmannsberger, C., Higano, C. S., Mukherjee, S. D., Gleave, M. E., Stewart, P. S. and Hotte, S. J. 2016, *Ann. Oncol.*, 27, 1116.
38. Massacesi, C., Di Tomaso, E., Urban, P., Germa, C., Quadt, C., Trandafir, L., Aimone, P., Fretault, N., Dharan, B., Tavorath, R. and Hirawat, S. 2016, *OncoTargets Ther.*, 9, 203.
39. Barone, F. C., Irving, E. A., Ray, A. M., Lee, J. C., Kassis, S., Kumar, S., Badger, A. M., Legos, J. J., Erhardt, J. A., Ohlstein, E. H., Hunter, A. J., Harrison, D. C., Philpott, K., Smith, B. R., Adams, J. L. and Parsons, A. A. 2001, *Med. Res. Rev.*, 21, 129.
40. Pignataro, G., Meller, R., Inoue, K., Ordonez, A. N., Ashley, M. D., Xiong, Z., Gala, R. and Simon, R. P. 2008, *J. Cereb. Blood Flow Metab.*, 28, 232.